Technical University of Denmark

DTU

Accuracy of depth of cut in micro milling operations

Bissacco, Giuliano

Publication date:
2003

Document Version
Publisher's PDF, also known as Version of record

Link back to DTU Orbit

Citation (APA):
Bissacco, G. (2003). Accuracy of depth of cut in micro milling operations. Institut for Produktion og Ledelse, DTU.

DTU Library
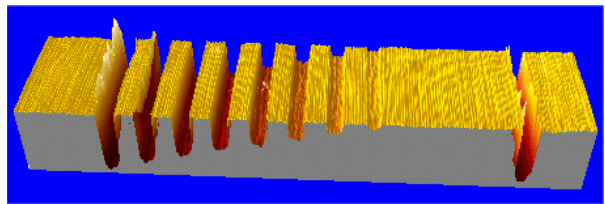Technical Information Center of Denmark

Accuracy of depth of cut in micro milling operations

Giuliano Bissacco   **2003**

MM   03.58

IPL   254.03

MANUFACTURING
ENGINEERING AND
MANAGEMENT

I P L

TECHNICAL
UNIVERSITY OF
DENMARK

DTU

Table of contents

Preface

This piece of work constitutes part of the experimental activities within the Ph.D. project Surface Generation and Optimization in Micromilling, carried on by Giuliano Bissacco under supervision of prof. Hans Nørgaard Hansen and prof. Leonardo De Chiffre. The report is concerned with the subject of machining accuracy in micromilling and presents an investigation for improving control of axial depth of cut in a conventional 3 axes CNC milling machine.

The author wishes to thank Pinol A/S and particularly Henrik Andersen for availability of facilities, Niels Sølling, Kasper Duus, Casper Beyer Larsen and Rolf Magnussen for their valuable assistance.

The author wishes to thank Fabrikant P.A. Fiskers Fond for the economical support provided to the project.

Accuracy of depth of cut in micro milling operations

1.   Introduction

In any kind of conventional machining operation, dimensional and geometrical accuracy of the machined part cannot be achieved without a precise control of cutting parameters as well as positioning accuracy. Miniaturization of components implies a reduction of all components' dimensions and involves downscaling of conventional manufacturing technologies. Although in micro manufacturing operations particular precautions are taken, the ratio between tolerances and absolute dimensions increases. However, the absolute required accuracy for the functionality increases, therefore the absolute value of tolerances decreases. Existing machine tools designed for conventional size machining operations are generally unsuited for mechanical micromachining due to a too low positioning accuracy and too high thermal deformations of the machine structure (while static and dynamic stiffness is not generally a problem since the magnitude of the cutting forces involved is reduced), which make mechanical micromachining by use of miniaturized tools troublesome or even impossible. This study deals with the use of a conventional 3 axis vertical milling machine equipped with a high speed attached spindle for micro milling operations, the identification of the main sources of inaccuracy and the solutions adopted for the optimization of machine performances through elimination or compensation of such inaccuracies.

2.   Situation in micro milling

When micro end milling is performed using a 3 axis vertical milling machine, the layout is the one presented in fig. 1 where the workpiece is clamped on the machine table and the tool and tool holder are fixed on the spindle. The spindle is connected to the table through the column, the ram and the slideways.
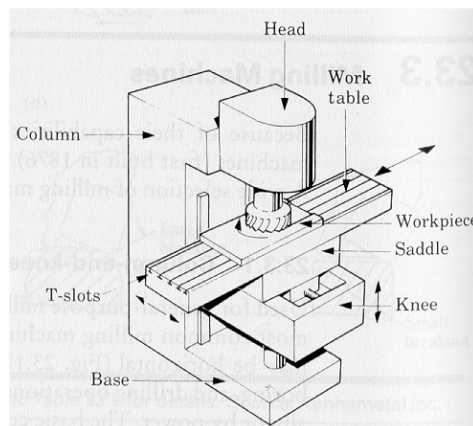
fig. 1 3 axis vertical milling machine

The features to be machined on the workpiece are generated by interference of the cutting edges of the rotating end mill with the workpiece material during the relative movement to each other. Many different types of milling modes and milling tools can be used, but in this work only end milling by use of flat and ball nose end mills is considered. The combination of the cutting parameters determines the dimension and geometry of the material removed from the workpiece and eventually the geometry of the manufactured part.
The nomenclature for the cutting parameters in flat end milling and in ball nose end milling is presented in fig. 2 and 3 respectively.

Flat end milling

The cutting action is performed on the periphery of the end mill on a cylindrical surface

View from the tool axis direction

View from the feed direction

f	feed rate [mm/min]
V	cutting speed [m/min]
n	rotational speed [rpm]
z	number of teeth
a_z	feed per tooth [mm/tooth]
a_e	radial depth of cut [mm]
a_p	axial depth of cut [mm]
θ	engagement angle [deg]
h [mm]	instantaneous chip thickness
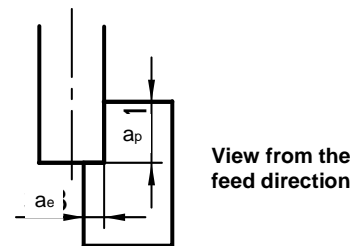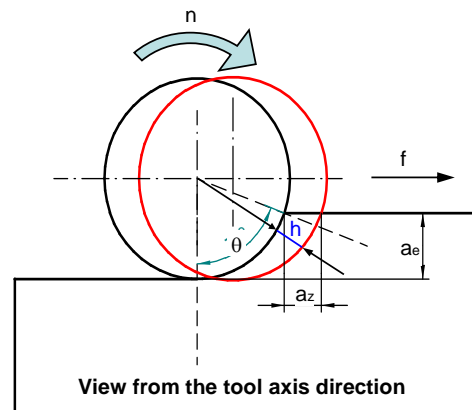
Fig. 2 Nomenclature of cutting parameters in side end milling.

Ball nose end milling

The cutting action is performed on the periphery of the end mill on a spherical surface
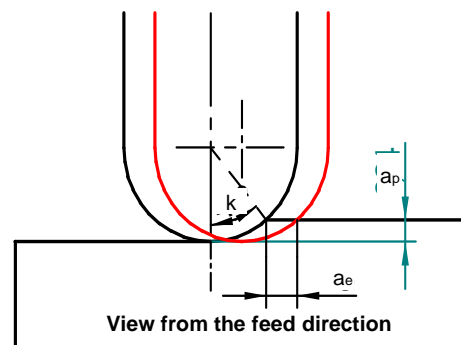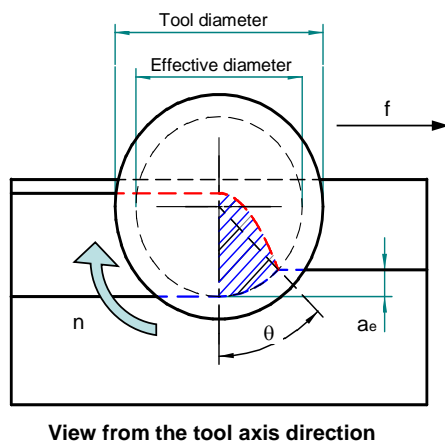
Tool diameter

Effective diameter

View from the tool axis direction

View from the feed direction

f	feed rate [mm/min]
V	cutting speed [m/min]
n	rotational speed [rpm]
z	number of teeth
a_z	feed per tooth [mm/tooth]
a_e	radial depth of cut [mm]
a_p	axial depth of cut [mm]
θ	engagement angle [deg]
k	axial immersion angle [deg]
h [mm]	instantaneous chip thickness

Fig. 3 Nomenclature of cutting parameters in ball nose end milling.

From a definition point of view, micro milling differs from conventional milling only by the size of the milling tools used. Some authors limit the range of diameters to less than 2 mm, while others prefer to identify the micro milling range as the submillimiter diameter range. Commercially available tungsten carbide end mills can have diameters down to 200 μm, cutting length of 300 μm and neck length of 1 mm. Compared to normal size end mills, these values are smaller by two orders of magnitude. It is expectable therefore that also the geometric cutting parameters are consistently reduced. Table 1 shows geometrical cutting parameters used by the author in micro milling of 58 HRC tool steel.

Parameter		Value
Tool diameter	D	200 μm
N° teeth	z	2
Feed per tooth	a_z	2 μm
Radial depth of cut (or step over)	a_e	10 μm
Axial depth of cut	a_p	10 μm
Engagement angle	ϑ	25.84°
Maximum chip thickness	h	0.87 μm

Tab. 1 Geometrical cutting parameters used on 58 HRC tool steel. Tool diameter 200 μm.

3.   Significance of precise settings in micro milling operations

From table 1 it is apparent that the precision of the settings necessary for smoothly running any micro milling operation is rather high. Considering the nominal capabilities of normal milling centres, it is apparent that local variations of the chip load of more than 100% are easily produced and, when the actual process is considered, overloads as high as 500% can occur unless particular precautions are taken. The difference between the nominal and actual process are due to finite static stiffness of the machine structure, low dynamic performance of feed drives, tool wear and tool deflections and thermal deformations of the tool, machine and workpiece, which are responsible for workpieces dimensional and geometric errors.

In micro milling operations, the static stiffness of the machine tool structure is not critical since the absolute values of the forces involved in the cutting process are very small, generally below 10 N in all directions and the mass of the workpiece is normally negligible (thereby influent inertia).

The dynamic performance of feed drives is instead a main concern since the relative positioning accuracy of tool-workpiece is definitely affected by the accuracy of positioning provided by the feed drives; moreover, bad acceleration and deceleration capabilities

along all axis, particularly when displacements are small and feeds are high, also contribute to the geometric errors of the machined part.

Tool deflections are generated by the forces involved in the cutting process; they can be negligible in some conventional size milling operations if the cut is rather light and the tool is very stiff, as is the case for short end mills with big diameters or face milling tools. However, in most of the end milling operations, the machinist must be aware of tool deflections, particularly when deep pockets are being finish milled, due to the disadvantageous proportions between tool length and diameter. In micro milling operations the situation is much worse, since the ratio between length and diameter becomes more unfavourable with size reduction. In fact, despite the desired diameter reduction, often the length reduction is limited by accessibility problems and the aspect ration of the part. Although the absolute value of the cutting forces reduces with diameter reduction, the relative deflection (deflection divided by the diameter) increases. Tool wear has also the effect of increasing the cutting forces, hence increasing deflections. The main effect of tool wear is an increased roughness of the generated surface and altered surface integrity. In addition wear reduces the tool diameter and eventually affects the dimensions of the workpiece.

Thermal deformations are the largest source of machining errors and can account for more than 100 μm. As mentioned above, in micro milling operations, the chip size and the material removal rate are very low and therefore little heat is generated and also the absolute dimensions of the workpiece are small. Moreover, if liquid lubrication is used, the distortions in the workpiece due to cutting process generated heat can be neglected. The relevant thermal deformations are therefore those concerning the machine tool structure, which most of the times is steel made and definitely not small. The problem of thermal distortion of machine tools is well known for conventional size machining operations and has been the subject of many investigations especially in the recent years.

From the short introduction to the main influencing factors on workpiece accuracy, the importance of precise control of the cutting parameters is apparent. When a conventional milling machine is intended to be used in connection with micro end mills, inaccuracy do not only affect the precision of the workpiece but might make the operation impossible. The loads the tool can withstand to are very small and bad control can easily generate high overloads. This in turn produces high tool wear, big tool deflections and tool breakage. Imprecise control of the tool position or small indetermination of the tool length in fact can cause the breakage of the micro tool at the first contact with the workpiece, thus making machining impossible.

With respect to this study, the precise control of the cutting parameters was particularly important since the investigation was based on a physical scale simulation of the milling process, which included a modular approach to the variation of the chip shape. Control of chip shape and size was realized through precise setting of axial and radial depth of cut, feed per tooth and rotational speed. Such an approach emphasized the accuracy requirements to the relative positioning and movement of tool and workpiece.

Different strategies can be used to keep a precise control of the parameters, but it should be noticed that the maximum accuracy achievable without a modification of machine parts or devices, corresponds to the positioning repeatability of the controller in the three axes.

4. Influencing factors on precision of cutting parameters and machining accuracy

In fig. 4 the influencing factors on the machining accuracy of an end milling operation are displayed, grouped in seven main groups which represent the *Independent Process Parameters* according to the general theory of machining. Machining accuracy is instead the only *Performance Parameter* considered here. To the five independent process parameters normally identified (workpiece, tool, machine tool, cutting fluid and process parameters), two more have been added, namely setup and environment. This is because these factors, become more important with workpiece and tool size reduction.
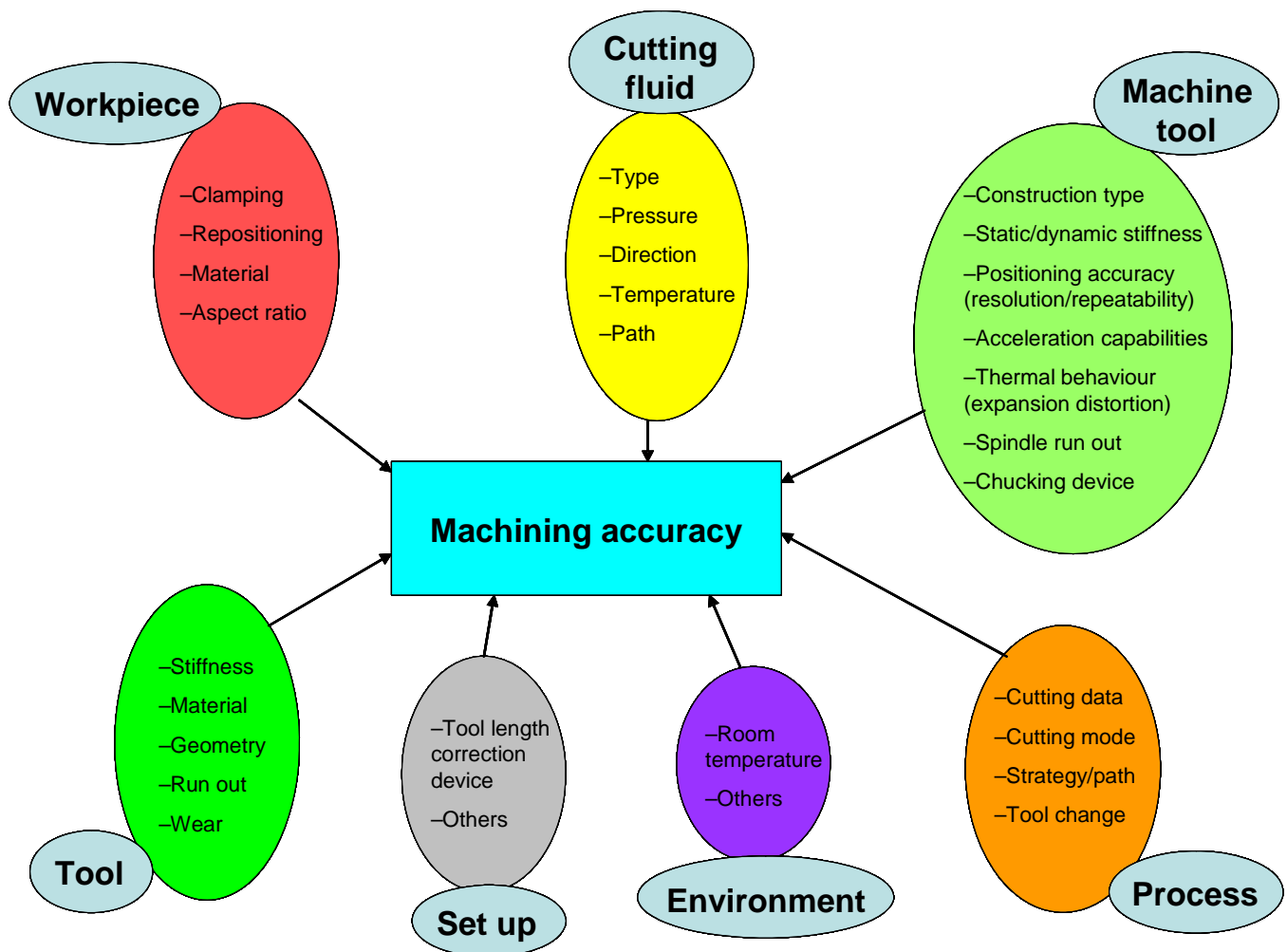
Fig. 4 Influencing factors in milling operations.

The relative weight of each factor changes with the overall size of the process and the type of operation to be performed. For the particular kind of operations for which this study was carried out, some of the influencing factors listed in fig. 4 can be neglected. For example, as mentioned above, the machine tool stiffness is no longer important when the forces are small; furthermore, when proper choices regarding tool and workpiece material and cutting data are made (or forced), the influence of these is reduced. After some

considerations, the most important factors influencing the relevant settings for this study where reduced to the following:

1. tool stiffness
2. tool wear
3. tool length correction device
4. overall run out (tool run out after chucking)
5. machine positioning accuracy
6. machine/spindle thermal distortion/elongation
7. coolant temperature
8. coolant pressure
9. room temperature

Unfortunately, the entity of the errors due to the above listed causes, were so high that micro milling operations with 0.2 mm ball nose end mills were impossible due to systematic breakage of the tools.

According to the modular approach cited above, the parameters to be controlled were the axial and radial depth of cut, by direct control of the relative position between tool and workpiece and the feed per tooth through the control of rotational speed and feed rate. While the degree of variability of feed per tooth and radial depth of cut only affected the process performance, the error on the control of the axial depth of cut was so bad that in ball nose end milling operations, systematic breakage was experienced when milling surfaces at low angle (0° to 10°).

Each of the nine factors listed above will be now singularly considered, in connection with the particular applications concerning this study, and the magnitude and direction of its contribution to the errors on the cutting parameters will be discussed. For those which behaviour is not random, a vector (magnitude and direction) will be then drawn and an overall error map will be sketched.

4.1   Tool stiffness

With the name *tool stiffness* we refer to the deflections of the tool produced by the cutting forces due to its finite rigidity. This is definitely not a random contribution to the machining errors. The magnitude and direction of the cutting forces depend on the geometry of the end mill and cutting mode (up or down milling) and vary along the engagement angle. Measurement of cutting forces in micro end milling is particularly difficult due to the very low force magnitude, the low signal-to-noise ratio and the high frequency, which require specially developed dynamometers and acquisition boards with high sampling rate, high sensitivity, very low noise and high resonance frequency. However several models have been developed for prediction of cutting forces in conventional size milling, for both flat end and ball nose geometry. Although these models are not directly applicable to micromilling, because of the many size effects introduced with miniaturization, they can be useful in determining the order of magnitude and the ratios between the different force components. Figure 5 shows the three force components as they result from the application of a model based on "Unified Mechanics of Cutting" [11] using the cutting data reported in tab. 1.
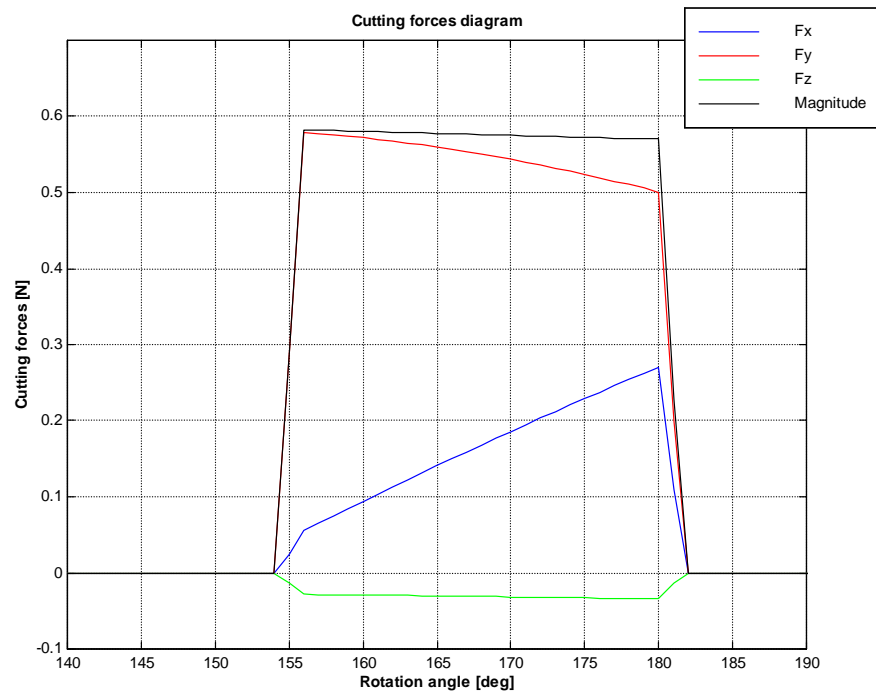
Fig. 5 Cutting force components in flat end milling calculated applying Altintas' model with the cutting data reported in tab. 1. X, Y, Z direction are oriented respectively according to feed, pick feed, and axial directions (see fig. 6).

The resulting force components, calculated at the angular position corresponding to the maximum radial force, are:

Fx = 0.0577 N,

Fy = 0.5788 N,

Fz = -0.0281 N

Ftot = 0.5822 N
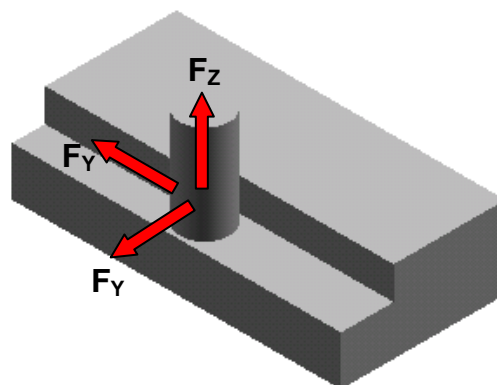
Fig. 6 Cutting force components and their orientation in flat end milling.

Elastic FEM simulations with the calculated values of the cutting force components allow calculation of the total displacement as well as displacement components. With the calculated force values, the displacements at the tool tip are:

$\Delta x =$ + 6.01 μm

$\Delta y =$ + 62.48 μm

$\Delta z =$ + 3.73 μm

Displacement magnitude = 62.87 μm
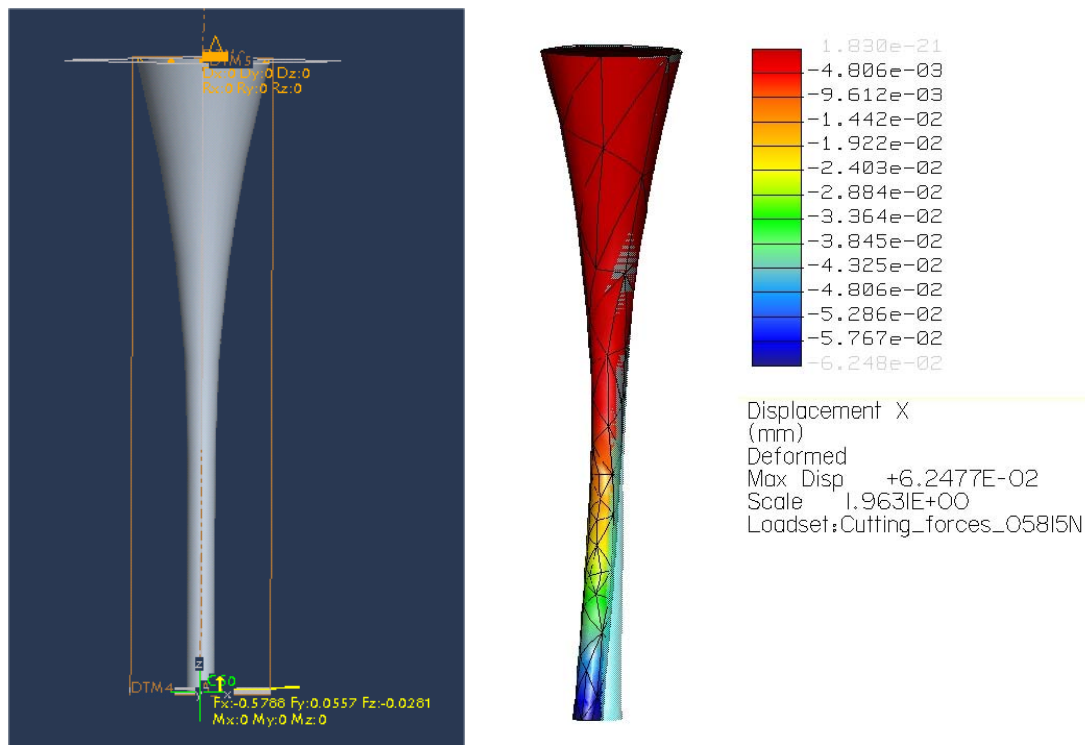
Fig. 7 Tool tip model and FEM result for tool tip displacement in X direction under the estimated load.

The calculated values of force and displacement components have to be intended as first approximation values due to the inaccuracies of the model with the reduction of the absolute dimension of the process. However it is noticeable that for the cutting parameter of table 1, and in absence of overloads, displacements of several tens of microns have to be expected. The same method can be applied to ball nose end milling, so that the order of magnitude of machining error of free form surfaces, due to tool deflection, can be estimated and the most critical points in the machining path can be identified.

4.2   Tool wear
The main effects of tool wear are to increase the cutting forces, therefore increasing the deflections, and to reduce the tool diameter and length therefore altering the workpiece dimensions. As a first approximation, the deviation due to tool wear can be accounted for as a fraction of the contribution due to the tool deflection. Tool wear becomes particularly important with process miniaturization, since smaller worn volumes determine bigger deviations from the ideal tool shape, critically affecting performances of the tool and integrity of the generated surface. Moreover, tool wear measurement is particularly difficult in micromilling, because of the small dimensions, and it requires high magnifications and long preparation time. Fig. 8 shows the comparison of the shape of a ball nose end mill before and after machining hardened tool steel; the tool diameter is 0.2 mm.
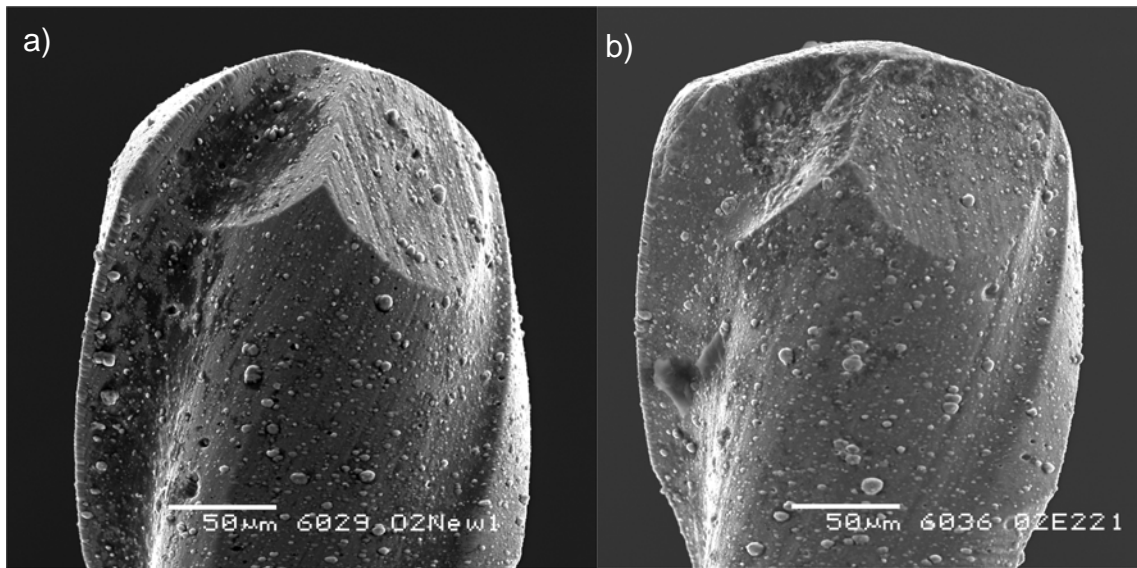
Fig. 8 0.2 mm ball nose end mill before a) and after b) machining hardened tool steel at different inclination angles. The comparison shows that tool wear highly affects tool geometry.

Due to the difficulties connected with tool wear estimation, and the fact that its contribution is variable during the process, the influence of tool wear on machining accuracy will not be taken into account here.

4.3   Tool length correction device
The device used for the tool length correction directly affects the accuracy of the axial depth of cut during machining. When using attached spindles, which are chucked into the main spindle in the same way as for tool holders, the automatic tool change is impossible and the tools have to be changed manually by insertion into the collet chuck. This prevents the possibility of presetting the tool length by off the machine measurement and introduces need for an on the machine tool length correction device. The accuracy of this device is sometimes difficult to estimate due to some influences not always completely understood. As a first approximation an accuracy of 5 μm can be assumed.

4.4   Overall run out
Run out after chucking refers to the rotation error of a calibrated shaft chucked into the spindle. This takes into account the effect of the rotational accuracy of the spindle and the misalignment of the shaft axis relative to the spindle axis due to chucking (see previous report for definitions). The run out of the tool teeth is not considered. The effect of this error is to increase the radial depth of cut. In the experimental investigations connected with this study, the measured run out was 5 μm at a distance of 40 mm from the collet cap.

4.5   Machine positioning accuracy
The machine positioning accuracy directly affects the machining accuracy. As mentioned above, not only the positioning repeatability but also the accuracy of the feed drives has to be taken into account. These errors can be regarded as random errors and therefore cannot be compensated for. As regards the present experiments, no machine tool tests have been performed, therefore a precise value for these errors cannot be stated. However, several machining tests with incremental depth of 1 μm have indirectly shown a good repeatability of positioning, which seems to be in the order of 1 μm. Also important for the machining accuracy is the straightness of the machine guides. During the tests, a

slight bend of the machine X axis slideways was discovered which accounted for a straightness error of 5 μm over a length of 90 mm.

4.6   Machine/spindle thermal behaviour

As recognized by many authors, this is the most serious and the most important source of machining errors. Internal and external heat sources create thermo-elastic deformation of the machine structure and in the end result in geometrical inaccuracies of the workpiece [1]. In [2] Bryan gives an overview of the problem dated 1990 and proposes the diagram reported in fig. 9 as a means of organizing the subject of thermal effects.
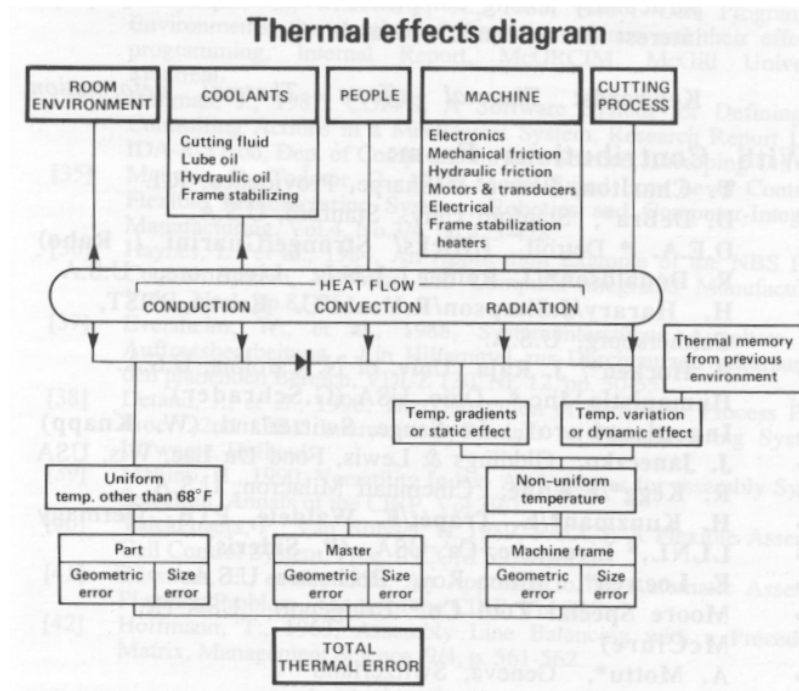
Fig. 9 Diagram showing the relationships between causes of thermal effects, heat transmission phenomena and effects as contribution to the total thermal error [2].

Different heat sources combined with different mechanisms of heat transfer lead to a uniform temperature other than 20 °C or to a non-uniform temperature distribution over the machine structure. The diagram also illustrate the concept that every machining operation consists of a three element system made up of the part, the machine frame and the scale.
In [1] the heat sources are divided in external and internal. External heat sources include the changes in environment as solar radiation, space heaters, lighting, etc. Internal heat sources refer to the heat produced by running the machine and the process itself.
The environment affects the three element system in a way that is not readily apparent. There would be no consequences of environmental temperature variation if all portions of the three element system had exactly the same coefficient of expansion, the same volume-to-surface ratio and the same density and specific heat. This is not the case in real systems. Thin sections having small volume-to-surface ratio respond faster than thick sections. Temperature variation affects the length of every object in a different way. This effect is called dimensional response. It is a function of the frequency of temperature variation. The difference in response between any two objects is called differential response. Differential response reaches a maximum at some particular frequency of temperature variation in a manner that is analogous to resonance in vibration work [2].

Equalising the time constants for components involved is effective in reducing thermal drift caused by external heat sources [1].

Internal heat sources instead have the effect of generating and conducting the heat into the machine structure, causing variation of overall temperature of machine parts and temperature distribution, leading to thermal drift and distortions.

One of the main sources in terms of its contribution to the total heat generation and resulting deformations is the spindle system and its bearings. Based on the thermal load, design and cooling conditions, the spindle and box growth in the axial direction can account for 100 μm or more [1]. Depending on the bearing type and on the spindle size, the power loss can be up to 100 W for a 100 mm ball bearing running at 10000 rpm and up to 1 KW for a hydrostatic bearing of the same size and rotational speed.

The feed drives of the machine are also major heat sources which can result in considerable thermal drift at the tool depending on the encoder system. Particularly, the ball screw and its nut are responsible for local increase of temperature up to 82°C [1].

The other important internal heat source is the cutting process itself which, in normal machining operations, warms up the tool, tool holder, workpiece and clamping device. The table of the machine and other components can be warmed up by hot chips. However, as already mentioned, this last contribution is missing in micro milling operations, since the thermal energy generated by the cutting process is very small and the chips have sizes in the order of few microns.

The solutions to the problem of machine tool thermal deformation can be grouped in three categories:

- reduction and insulation;
- temperature control of machine tools;
- compensation.

Reduction of the power loss due to internal heat sources and their insulation involves redesign of the machine tool or some of its parts. The power loss of spindle bearings can be reduced by optimizing the lubrication, by using new materials for the balls and by optimizing the preload [1]. Hybrid bearings with ceramic balls have less friction than conventional bearings under the same conditions. Lubrication of the bearings through small drillings in the outer ring of the bearings increases the quality of lubrication and leads to higher permissible speeds with smaller temperature rise. The preload of the spindle system has significant influence on the friction torque and therefore on the power loss. Spindle bearings must be preloaded for achieving the necessary stiffness for machine tool applications. The insulation of the bearings from the spindle has proved to be an effective method for spindle elongation reduction. Particularly, the use of a ceramic spindle and a carbon reinforced plastic spindle instead than a conventional steel spindle resulted in a reduction of the axial thermal drift respectively by a factor 7 and by a factor of 15. Studies on machine tool structures made of concrete are reported in [1]. The advantage of concrete is its low thermal diffusivity and therefore an higher time constant of the machine tool can be achieved, that means rapid changes of internal and external heat sources cause lower distortions (the machine tool structure is less thermally responsive).

Many examples of *temperature control of machine tools* have been reported in the literature. Extremely sophisticated systems for temperature control have been developed in the last years. Oil and air showers over the machine and heat pipes have proved to be effective for reduction of thermal deformation of machine tools.

Techniques for _compensation of machine tool thermal behaviour_ are generally subdivided into direct and indirect compensation. For the direct compensation, the drift displacements between the tool and the workpiece are directly measured, while the indirect compensation uses a model so that signals correlating with the drift values are used to calculate the displacement via the mathematical model.

Direct compensation is often difficult because this implies a periodic measurement of machine distortions during machining. However some examples are reported in the literature. Furthermore probing units for machine tool applications are commercially available for use on CNC machining centres and lathes. The tool can periodically touch this units to establish tool wear and thermal drift. An efficient way for direct compensation is the measurement by use of laser beams to establish the position of the tool relative to the workpiece table.

Indirect compensation requires the measurement of the temperature at representative points in the machine tool structure as a function of time. These temperature measurements constitute the input for the mathematical model which can be either theoretical or empirical. The calculated distortions are then either compensated by use of the CNC or by additional special built-in actuators. Spur et al. [5] discussed the limits of indirect compensation when the temperature is measured only in few points of the machine tool. They argue that although it is impossible to compensate exactly with only a few measuring points, a tolerable error is made if the significant temperature locations are found. Therefore, finding the significant temperature points is of the utmost importance for indirect thermal compensation. Yet, only those locations which are actually significant should be included; an oversized number of temperature points means in fact an increased number of sensors and increased computational time. According to Weck et al. [1], the main interest of research activities world wide is directed to the question of how to find an acceptable mathematical model with a minimum temperature sensors within an acceptable time scale.

Concerning the problem addressed in [1], it is the author's personal experience that empirical calibration under fully repeatable conditions can potentially lead to very precise control even with few or single point temperature measurement. This is because if boundary conditions are fixed and repeatable, a kind of sub-space for the solutions to the distortions problem is isolated and eventually, a univocal relationship can be found. This concept will be better clarified later on in the present report.

The approach most used so far is that of measuring relative linear and tilt motions between the spindle and the table while, at the same time, the temperature is measured at different points in the machine structure and the environment. Performing a wide range of duty cycles, a wide range of temperature changes over the structure of the machine tool is generated and sufficient input data are therefore provided. A linear equation system is built with the provided data and using regression analysis, the best fit mathematical description of the machine thermal behaviour, with respect to the measured data in the teaching phase, can be found.

Artificial Neural Networks have been extensively used in the last 10 years. Neural Networks are capable of estimating the deformations very precisely when they are trained with data of the same operational conditions. They can also estimate the deformations under different conditions, but the accuracy depends on the range of variations in the training data. Neural Networks have been used in [6] also to identify significant temperature points by automatic deletion of the inputs from the temperature points which show to have small influence.

What presented in this paragraph shows that in order to reduce thermal errors in machine tools and maintain a very precise control of spindle-table relative position, compensation alone is not sufficient and needs to be combined together with temperature control

systems and sensible design. However, compensation accounts for a reduction of the thermal drift by up to 90%.

4.7   Coolant temperature

Except for machining operations performed dry, the activation of the coolant constitutes a thermal shock for the whole machine structure. In fact, during machining, the coolant hits the table and the structure of the machine tool and generally the temperature of coolant and machine structure differs by several Kelvin at the moment of coolant activation. Therefore after activation the temperature of both coolant and structure tend to reach an equilibrium. If the coolant is colder than the machine frame, the latter will decrease its temperature and will contract according to the law of thermal expansion and the former will warm up. The opposite happens if the fluid is warmer. Moreover, due to the power given to the fluid by the pump for recirculation and in case of conventional machining also by the hot chips produced, after a first quick variation, the fluid temperature increases with time, inducing a subsequent further thermal drift of the machine structure. Summarizing, the effect of the coolant on the machine frame results in a first, rather quick, temperature variation, followed by a slow temperature drift. The distortion of machine tool frame due to coolant action is manifold, as for the effects of other thermal sources discussed above. However, it influences particularly the relative position of spindle and machine table in Z direction. Therefore the cutting parameter most heavily affected in a 3 axes milling machine is definitely the axial depth of cut. When the tool length is preset before the activation of the coolant and, as is usually the case, the coolant is colder than the machine frame, the temperature of the machine column decreases and the column becomes shorter. Thus the distance between the table and the tool decreases and the axial depth of cut increases. The diagram in fig.10 shows qualitatively the effect of the coolant on the axial depth of cut.

Fig. 10   Qualitative effect of the coolant temperature on the axial depth of cut by intermittent coolant application (here the coolant is supposed to be colder than the machine frame).

A solution to this problem is of course dry machining, but for those operations where either lubricant or coolant is necessary, a very accurate control of cutting fluid temperature, in order to minimize the temperature difference with the machine column, would reduce the problem. However this implies higher initial cost of the machine tool. A rougher but inexpensive solution would be the continuous use of coolant, even during set up phases.

By doing so, after a first transient period when the fluid and machine temperatures equalize, the system can be considered stabilized and only the thermal drift caused by the slow increase of fluid temperature, due to the power given to the fluid by the pump, will still be present. Therefore, if tool length correction is performed after stabilization, the axial depth of cut will increase, owing to the cutting fluid, only slightly and slowly. Fig. 11 shows the situation in this case.
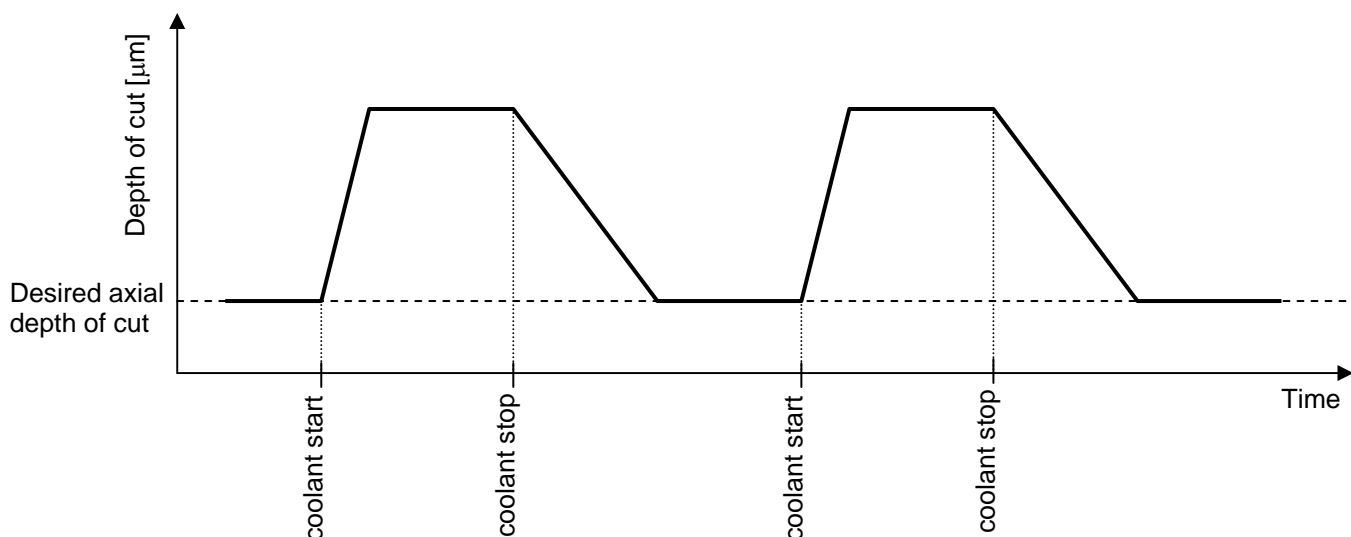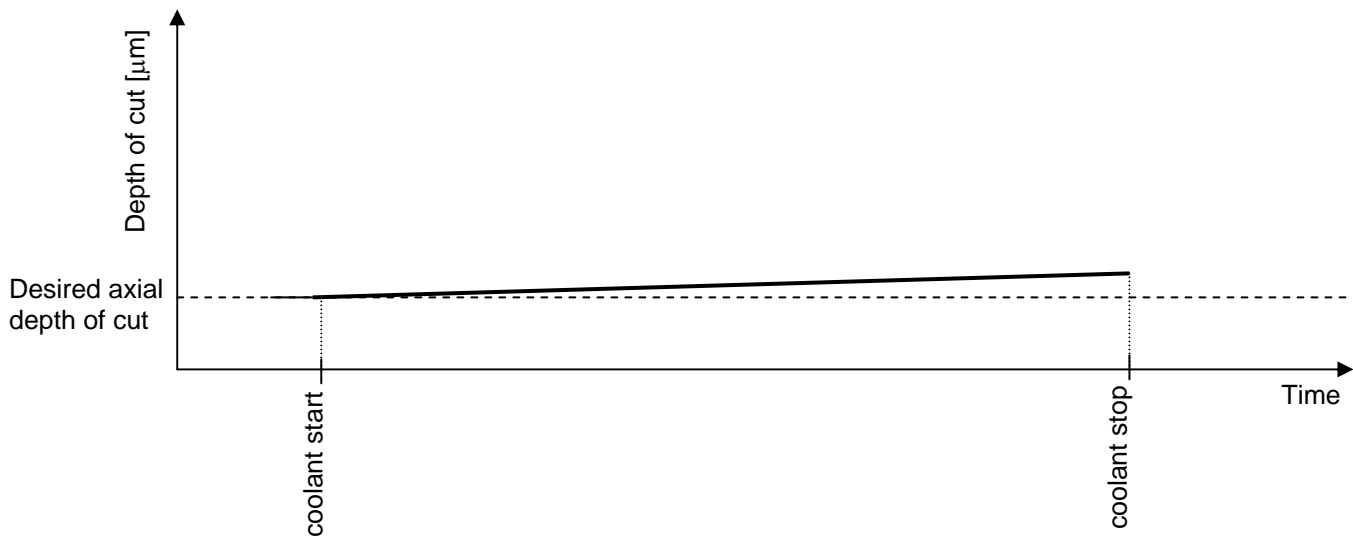

Fig. 11   Qualitative effect of the coolant temperature on the axial depth of cut by continuous application (here the coolant is supposed to be colder than the machine frame and tool length correction is performed after pseudo-stabilization).

This last solution is the one that has been used in the experiments connected with the present study. The relevant tests and their results will be presented and discussed later in this report. Anyways the deviation of the axial depth of cut in a 3 axes milling machine can be reduced by more than 10 μm by using this method.

4.8   Coolant pressure

The pressure of the cutting fluid is provided by the pump present in the coolant flow system and is typically in the order of 6 bar at the exit of the pump. Assuming that half of this pressure is lost by flow resistance in the hydraulic circuit and that the speed at the exit from the pipeline is negligible, the total energy of the fluid at the exit from the pipeline is constituted by the pressure energy corresponding to a pressure of 3 bar. In conventional size machining an increase in coolant pressure is beneficial since it assures a more effective evacuation of the chips from the flutes of the tool, so that tool temperature is kept lower. The pressure is never high enough to generate accuracy problems. This is clearly not the case in micro milling. The tiny end mills are lacking in strength and stiffness and the dynamic pressure built up at the lateral end mill surface can generate deformations which are not negligible depending on the size and aspect ratio of the end mill. The model and the results from a numerical simulation, used to calculate the deformation in a flat end mill of 0.2 mm in diameter and 1.5 mm in constant diameter length, are shown in fig. 12. The applied pressure was 3 bar, estimated on the basis of the above discussion. The resulting maximum displacement in the direction of the coolant flow is 4.82 μm at the tip of the tool. This is not a negligible contribution to the overall accuracy and therefore needs to be considered. Moreover the direction of the displacement depends on the direction of

application of the coolant which can be chosen in order to minimize the effect on workpiece accuracy. For instance, a direction orthogonal to the machined surface can be used to reduce the deflection of the tool due to the average cutting force.
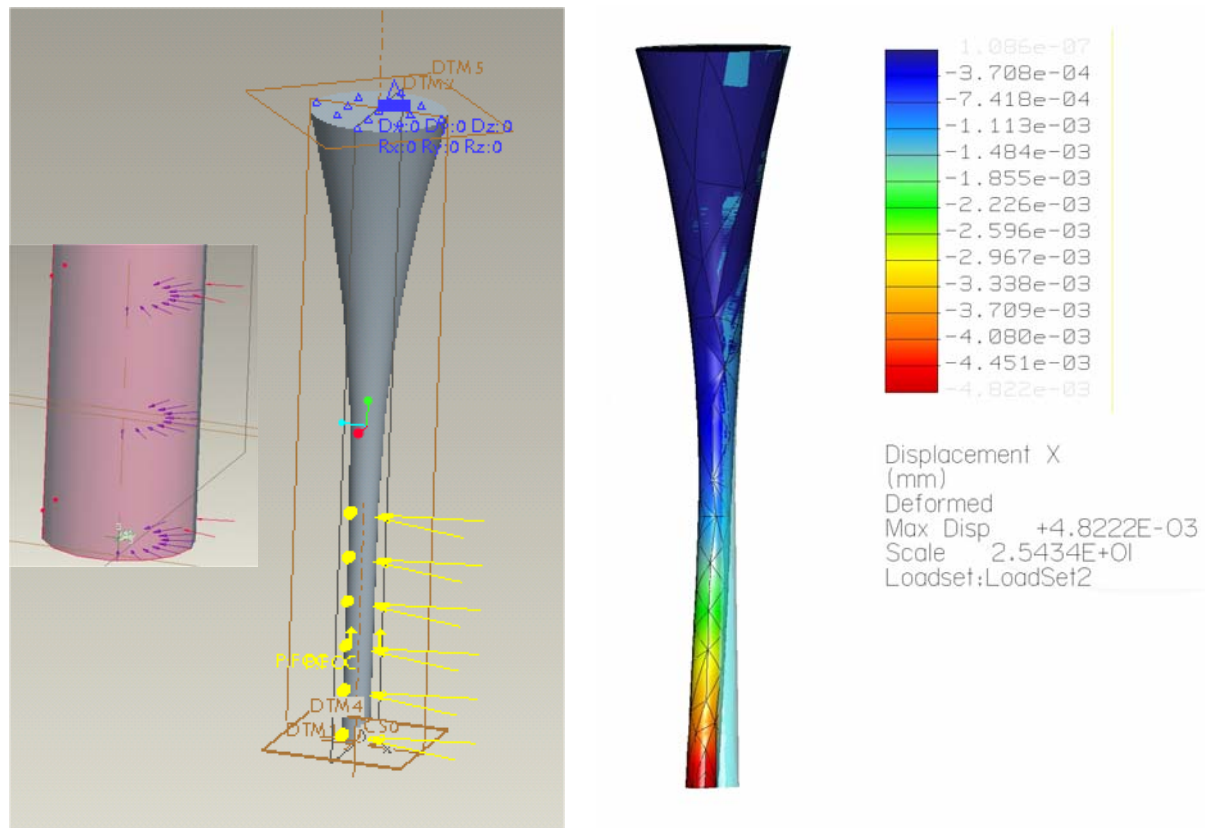

Fig. 12 Simulation results for coolant pressure of 3 bar on a 0.2 mm diameter tungsten carbide flat end mill. Left: simulation model and close up view of the pressure loads. Right: calculated displacements along the coolant application direction. Maximum displacement at the tip is 4.82 μm.

4.9   *Room temperature*
Room temperature variations are among the factors responsible for thermal deformations of the machine tools and in this respect their effect falls within the subject treated in the previous section *Machine/spindle thermal behaviour*. However, due to the kind of optimization procedure applied in the present work for accuracy improvement, temperature variations of few degrees may introduce further inaccuracies. Since temperature distribution is definitely not uniform, machining accuracy is affected not only by the average spatial temperature, but also by the temperature spatial gradients. The actual range of variation of average room temperature and spatial gradients, depends on the workshop environment where the machining is carried out. Environments without temperature control are subjected to seasonal and daily average temperature changes, with a range up to 20°C. Horizontal temperature gradients are produced by local heat sources, while vertical temperature gradients are generated by solar radiation and by the variation, with temperature, of the air specific weight. Therefore the temperature distribution within a machine shop depends on its location and height. Differences of local temperature of more than 5 °C can be observed in normal workshops. Workshops dealing with precision machining have generally temperature control with a variation range of ± 2° C and spatial thermal gradients are consequently also reduced.

4.10   Summary

As stated above, the aim of the discussion taken along paragraph 4 was to estimate direction and possibly magnitude of the contributions to the overall machining errors provided by the causes taken into consideration. The following table summarizes the results for the 0.2 mm flat end mill.

Contribution	Error [μm]		
	X	Y	Z
Tool stiffness	up to 63	up to 63	up to 4
Tool wear	---	---	---
Tool length correction device	No influence	No influence	5
Overall run out (after chucking)	5	5	No influence
Machine positioning accuracy	1	1	1
Machine/spindle thermal distortion/elongation	---	---	up to 50
Coolant temperature	---	---	up to 10
Coolant pressure	up to 5	up to 5	No influence
Room temperature	---	---	---

Tab. 2   Summary of the error contributions due to the factors considered in paragraph 4. Tool diameter 200 μm; machine tool and equipment according to description in chapter 5.

5   Experimental setup

The basis for this investigation was a 3 axis vertical milling machine equipped with an electrically driven high speed spindle attachment, capable of 50000 rpm, and plugged into the machine main spindle using the taper fit. This and the next sections are meant to describe respectively the setup and the initial procedure applied to the experiments connected with this study, while section 7 will describe the modifications introduced in order to improve the accuracy and make the micro milling process possible.

5.1   Machine tool

 The machine tool used was a Deckel-Maho DMU 50 T, which is a vertical milling machine with 3 CNC controlled axes. A manual swivel rotary table provides 2 more axes with manual control. The design is a traversing column type and movements connected with the three CNC controlled axes are owned by the machine head, while the those connected with the 2 manually controlled axes belong to the table. All the movements are provided through centrally lubricated ball screw spindles and recirculating roller guide ways. The measuring systems are linear encoder type. Among other features, the DMU 50 T has a work area of 500/400/400 mm (x/y/z), speeds of up to 9,000 rpm, as well as a rapid traverse speed of up to 12 m/min and a feed velocity of 10,000 mm/min. The machine

control system is Heidenhain MillPlus CNC PILOT 1290. The following table summarizes the machine tool characteristics.

Characteristic	Measuring unit	Magnitude
X axis	mm	500
Y axis	mm	400
Z axis	mm	400
Speed range up to	rpm	9,000
Main drive (100/40% duty cycle)	kW	9/13
Feed rate	mm/min	10,000
Rapid traverse X/Y/Z	m/min	12
Tool magazine	capacity	16
Tool mounting		ISO 40
Control		MillPlus CNC PILOT 1290

Tab. 3 Characteristics of machine tool Deckel-Maho DMU 50 T.

5.2   High speed attached spindle

In order to provide the necessary rotational speed required for effective machining with the smallest end mills, an electrically driven high speed attached spindle was mounted on the taper fit of the machine main spindle. The rotational speed provided by the main spindle was in fact limited to 9000 rpm and was insufficient for the purposes of the experiments. The attached spindle was a NSK-Nakanishi HES-BT 40 H with maximum spindle speed of 50000 rpm. Such a spindle is constituted by a very compact brushless motor directly connected to the spindle. Motor and spindle are assembled together in a steel construction and this assembly is then inserted in a steel holder which interfaces with the main spindle and fits into the taper fit. The power is supplied to the motor by an external control unit through a connecting cable that inserts into the accessible part of the spindle holder. The spindle is provided with ultra-precision ceramic bearings in order to reduce the heat generation by friction; furthermore, to protect the motor, air cooling with air pressure of 2 to 6 bar is provided by means of a flexible plastic pipe that inserts into the spindle holder the same way as for the power cable. The maximum output power of the spindle is 195 W and maximum torque is 0.06 Nm in the range from 0 to 30000 rpm. Spindle run out is declared to be less than 1 μm when measured at the tapered part on the inside diameter of the chuck engaging portion. Run out after chucking as declared by NSK was less than 8 μm; this has been checked and resulted to be 5 μm at a distance of approximately 40 mm from the collet cap. Tool mounting is manual by use of two spanners and, by changing the collet chuck, tools with shank diameters from 0.8 mm to 6 mm can be mounted. The control unit was NSK-Nakanishi type NE52-500. It allows selection of the rotational speed with a resolution of 1000 rpm as well as the direction of rotation. The speed control was based on the detection of the motor feedback signal so that the displayed speed was the actual one even under loaded condition. Nevertheless, speed adjustment with resolution of 1000 rpm was a too coarse one for the purposes of the experiments. Thus, a multituning potentiometer has been substituted to the existing potentiometer used for speed adjusting. The potentiometer voltage signal has been calibrated against rotational speed detected by use of a laser tachometer and a digital voltmeter. The fine adjusting of the rotational speed

was then obtained using the potentiometer voltage signal. The following table 4 summarizes the spindle characteristics.

High speed attached spindle	
Spindle type	HES-BT40 H
Control unit	NE52-500
Max speed	50000 rpm
Max output power	195 W
Max torque	0.06 Nm (from 0 to 30000 rpm)
Spindle run out	< 1 μm
Run out after chucking	< 8 μm
Motor cooling	Air cooling 2-5 bar
Bearings lubrication	Life lubricated
Motor cooling	Air cooling

Tab. 4 Characteristics of High speed spindle NSK-Nakanishi HES-BT40 H.

5.3   CAD/CAM
All the tool paths used in these experiments were obtained by use of Mastercam CAM software on models created in Pro/Engineer.

5.4   Tool length correction and tool change
In this study, in order to record the tool length, which is one of the input parameters to the machine control, an inductive displacement sensor with resolution of 0.1 μm has been placed on the machine table, with its axis in vertical direction. A large flat probe having a flat surface in sintered carbide with diameter of 10 mm was mounted on the sensor. A reference system G57 in the machine computer has been set to identify the position of the probe's centre in X and Y; in Z direction the zero point was the position where the zero of the inductive probe's travel had been set. The device is shown in fig. 7.
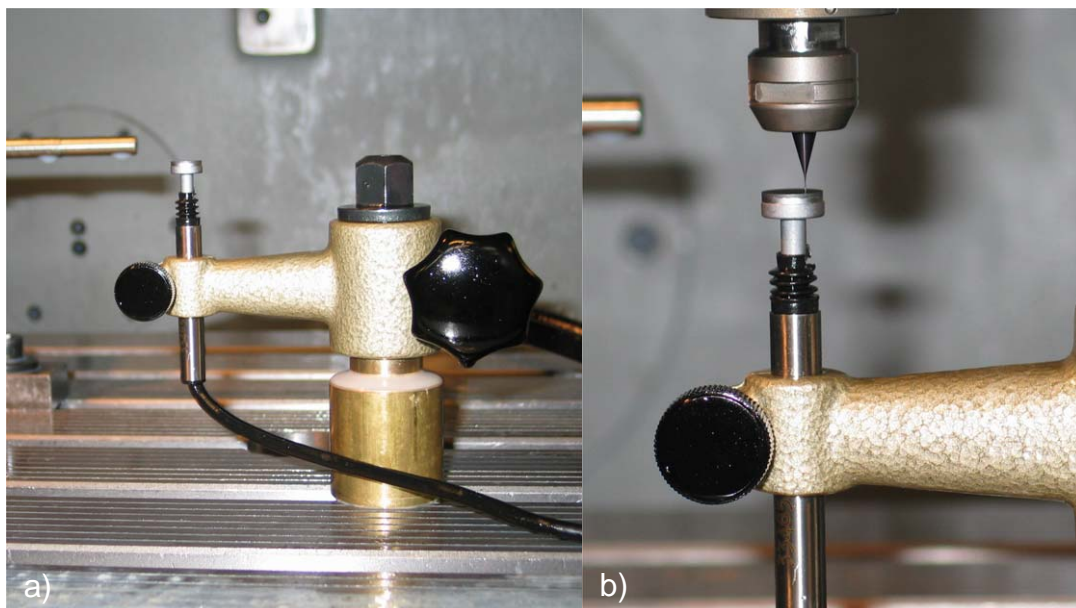

Fig. 7 Inductive probe for tool length correction a) and tool length correction phase b).

The tool length correction procedure after every tool change was as follows:

1. the tool is changed;
2. the reference system is changed to G57;
3. the machine head is driven to X=0, Y=0 (command G0 X0 Y0);
4. the tool is driven to the Z position where the TESA module displays 0.0 μm;
5. in the machine, for the reference system G57, this position is set to Z=0 and automatically the machine records the new tool length.

The new tool length is then used in all the operations until the tool is changed or a new tool length correction is performed.

Small misalignments of the inductive probe's axis relative to the spindle axis are easily generated when placing the probe on the machine table; however, if the tool diameter is the same for a series of operations and the zero point of the inductive probe is maintained at a constant position of his travel, the problem is not so critical. Nevertheless, when the workpiece surfaces are generated by means of different tools, errors are introduced. In this study, a 6 mm diameter flat end mill was used for generation of the reference surface of the workpiece and subsequently, micro end mills were used for the surfaces which were the object of the investigation. The worst case was that with the smallest end mill diameter (200 μm). Fig. 8 qualitatively shows the problem due to the misalignment of the inductive probe relative to the tool axis when different tool diameters are used.

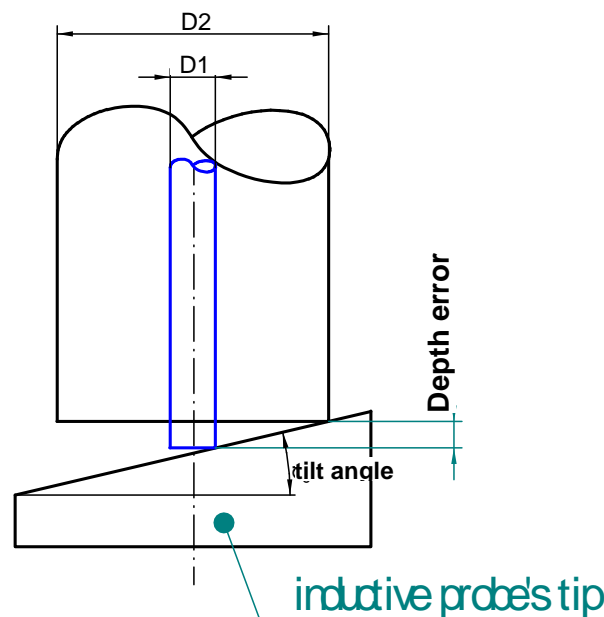Fig. 8 Effect of the misalignment between spindle axis and inductive probe when using different tool diameters.

A series of tests, carried out in order to isolate the contributions to the error on the axial depth of cut in the present study, have shown a misalignment of 0.107° which corresponds to an error in the axial depth of cut of up to +5 μm (positive contributions are those which effect is to increase the depth of cut).

5.5   Workpiece clamping

The workpieces were firmly clamped on a constant torque vice. Control of the clamping torque is useful when workpiece deformations can be introduced by the clamping system.

5.6   Cutting fluid

A 5% oil emulsion was used as cutting fluid. During non working time the fluid was stored in the reservoir underneath the machine tool. With regard to these experiments, the cutting fluid was necessary to provide lubrication more than cooling, since the cutting speeds were rather low an never higher than 30 m/min. It influences surface finish and, through its tendency to avoid built up edge, also workpiece accuracy. It shouldn't affect the accuracy of the cutting parameters set. However, since the cutting fluid flows over the machine table and the machine column during the process and its initial temperature differs from that of the machine parts, it induces thermal deformations of the machine tool as discussed above.

5.7   Environment

The working environment where the present work has been carried out was a machining workshop, equipped with air conditioning system for temperature control. The nominal temperature range was ± 2 °C. Such a working condition minimized daily and seasonal temperature variations as well as temperature spatial gradients, with consequent reduction of the related machine tool distortions.

5.8   Tool types

Tool geometries were flat end mills and ball nose end mills, both in TiAlN coated micrograin Tungsten carbide, with diameters of 1.0 mm, 0.6 mm and 0.2 mm.

5.9   Specimens geometry

Surfaces to be machined were flat surfaces with different inclination angles. The workpiece geometry is extensively described in a separate report.

5.10   Milling strategy

Milling strategy used in the present work was upward contouring, down milling. This is also described in a separate report.

6   Initial working procedure

Without going too much into details with the description of the specimens and their purpose, which is the subject of a separate report, it can be said that regardless of the material and workpiece/tool geometry, the initial working procedure was the same. At the beginning of the working day, the machine was turned on and a warming up cycle identical to one of the roughing cycles was repeated several times, with no load and a rotational speed of 30000 rpm, for a total of 1 hour. The workpiece was then clamped on the machine vice and no repositioning was allowed until the end of the machining cycle. The reference surfaces were produced in a roughing operation with a 6 mm diameter end mill and the "functional" surfaces were subsequently produced with an end mill of 0.2 to 1 mm in diameter. After the warm up, the roughing tool was manually mounted on the spindle chuck and the tool length correction was performed according to what reported in paragraph 5.4. Then the reference surfaces were generated and the tool again manually changed. So the micro end mill was mounted and again the tool length correction was performed in the same way as for the first tool. At this point the finishing operation, that is the machining of the functional surfaces with the second end mill was performed and,

depending on the cutting parameters, this second operation lasted from 20 minutes to 2 hours.

Unfortunately, the warming up cycle was not enough for the thermal stabilization of the machine tool-attached spindle system so that, together with some other inaccuracies introduced during the tool length correction phases, this led to systematic breakage of the 0.2 mm ball nose end mills, during machining of surfaces in hardened tool steel with an inclination angle of 10°. The breakage occurred because of a systematic over engagement of the tool into the workpiece, caused by an error in the axial depth of cut which was then more than 5 times the set value. The magnitude of the depth of cut error was higher than expected and discovered only when using the smallest ball nose end mills. For the larger ball nose end mills instead, the strength of the tools was high enough to withstand the overload and, as it will be shown later, since the over engagement increased with the rotational speed, which was lower for the bigger diameters, a smaller over engagement occurred and the overload was therefore only a reduced percentage of the ordinary chip load. When using flat end mills the problem was not critical because the thermal deformations occurred in a relatively long time and the increase of depth of cut between two subsequent passes was therefore negligible (the tool passes were in vertical sequence).

By means of a series of tests that will be illustrated in the next chapter, it was demonstrated that the error in the axial depth of cut was almost 40 μm. This magnitude of the error was not known when the breakage problem first occurred, but still the value of 40 μm has to be regarded as rather small when compared with maximum errors due only to thermal deformations occurring in normal machine tools which can be as high as 100-150 μm.

In the following, the series of tests performed for isolation and identification estimation/measurement of error contributions to the value of the actual axial depth of cut will be presented.

7   Isolation, identification and compensation of axial depth of cut error contributions

As mentioned above, the initial working procedure was affected by several error contributions to the axial depth of cut. Since a machine tool warm up with spindle rotating at 30000 rpm was routinely performed, and still systematic breakage when engaging the surface at 10° was present, it didn't seem obvious at all what the contributions were and how to solve the problem. As it will be shown in this chapter, the small thermal time constant of the attached spindle was the main reason for the breakages and for the difficult understanding of the problem. Tool deflection was instead the reason why breakage never occurred when milling surfaces at 70°. Due to the initial scarce understanding of the phenomena involved, tests sometimes have shown to be not completely meaningful but as they all concurred to outline the complete picture, they will be all reported in the following, in the order they have been carried out.

The different optimization phases regarding the accuracy of the depth of cut were in sequence:

1. Thermal stabilization of the machine by keeping the coolant always on;
2. Identification of the inclination angle between the spindle axis and the normal to the surface of the tip of the inductive probe;

3. Calibration of the high speed spindle expansion at different speeds.

The series of tests made in order to improve the depth of cut control was:

1. Identification of the thermal drift over time of the machine tool structure due to cutting fluid application;

2. First verification of the drift of the depth of cut over a period of 1 hour after compensation for the error due to the cutting fluid application;

3. Scanning the inductive probe tip for identification of the inclination of its surface;

4. Second verification of the drift of the depth of cut over a period of 1 hour after correction for the tip inclination angle;

5. First series of steps machined in Elmax with a height difference of 5 μm from +30 μm to -15 μm from the reference surface, to verify the capability of the 0.2 mm tool to withstand the 10 μm depth of cut. Compensations for coolant and tip were adopted;

6. Identification of the high speed spindle thermal drift, calibration of its expansion for different speeds and development of a compensation procedure;

7. Second series of steps machined in Elmax with a height difference of 5 μm from +30 μm to -15 μm from the reference surface, to verify the improvements in depth of cut control with the developed procedure. Compensations for coolant and tip were adopted;

8. First series of grooves with depth difference of 1 μm, from +5 μm to -5 μm from the reference surface, to verify the improvements with the above mentioned procedure without wear effects;

9. Second series of grooves with depth difference of 1 μm, from +5 μm to -5 μm from the reference surface, to verify the improvements with the above mentioned procedure without wear effects and reducing the misalignment error on the inductive probe caused by to axial run out of the roughing tool.

7.1   Identification of the thermal drift due to the coolant activation

Since the only thing which was not present in the warm up cycles was the coolant, the first thought was that the activation of the cutting fluid produced a rather quick variation of the temperature and temperature distribution on the machine tool structure. This thought was strengthen by the fact that the thermal capacity and the thermal convection coefficient of the cutting fluid are much bigger than those of air. The objective of the present test was to quantify the influence of cutting fluid activation on machine tool deformation.

Test description

In order to isolate the contribution due to the cutting fluid activation, the warm up routine was avoided. Therefore the machine was started at the beginning of the working day and a ball nose $\varnothing$ 6 mm end mill was mounted on the chuck of the high speed spindle. Then the tool length correction was performed and the machine head was intentionally left with the tool on the inductive probe's tip in the zero position in Z direction. At this point the cutting fluid was activated and the display of the inductive probe, which then corresponds to the apparent tool elongation, recorded during a period of more than one hour at regular

time intervals. Moreover, in order to validate possible conclusions, the temperature in different points of the machine tool structure (where it was hit by the cutting fluid) has been measured before and after the test. The temperature of the cutting fluid has been recorded during the test as well.

Results
The following diagrams show the apparent elongation of the tool, measured in terms of the displacement in Z direction induced on the inductive probe, due the application of the cutting fluid over a period of 65 minutes and the variation of the temperature of the cutting fluid during the same period of time.
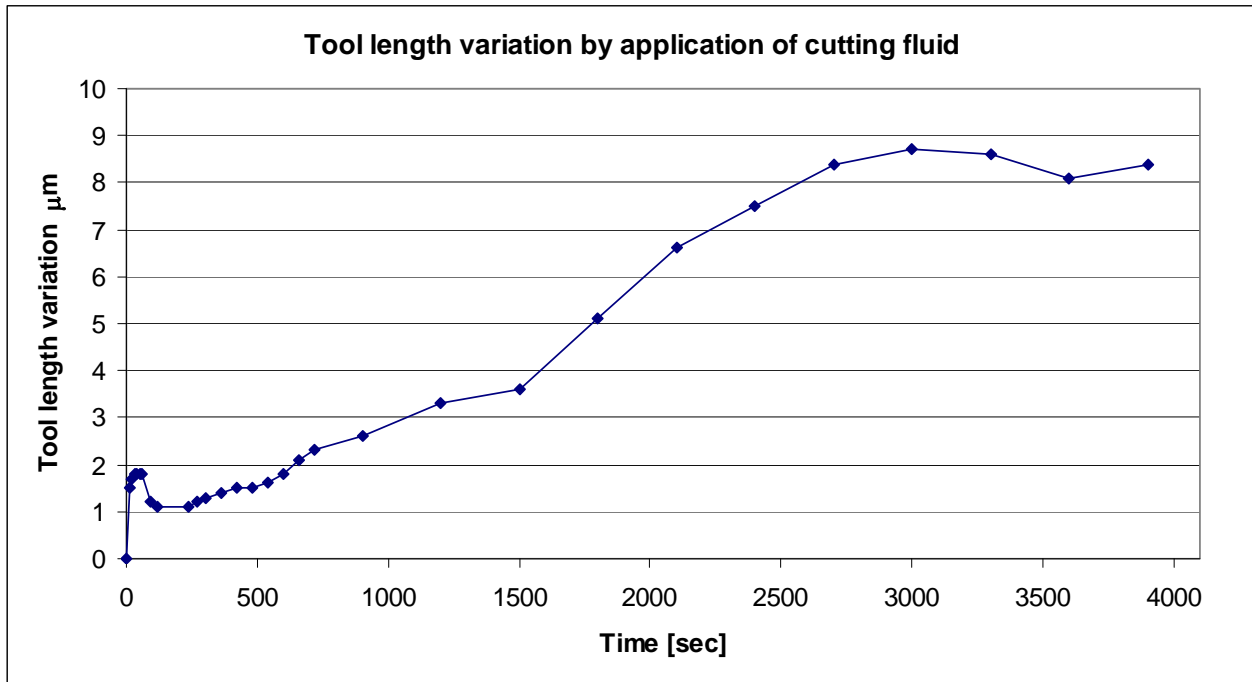

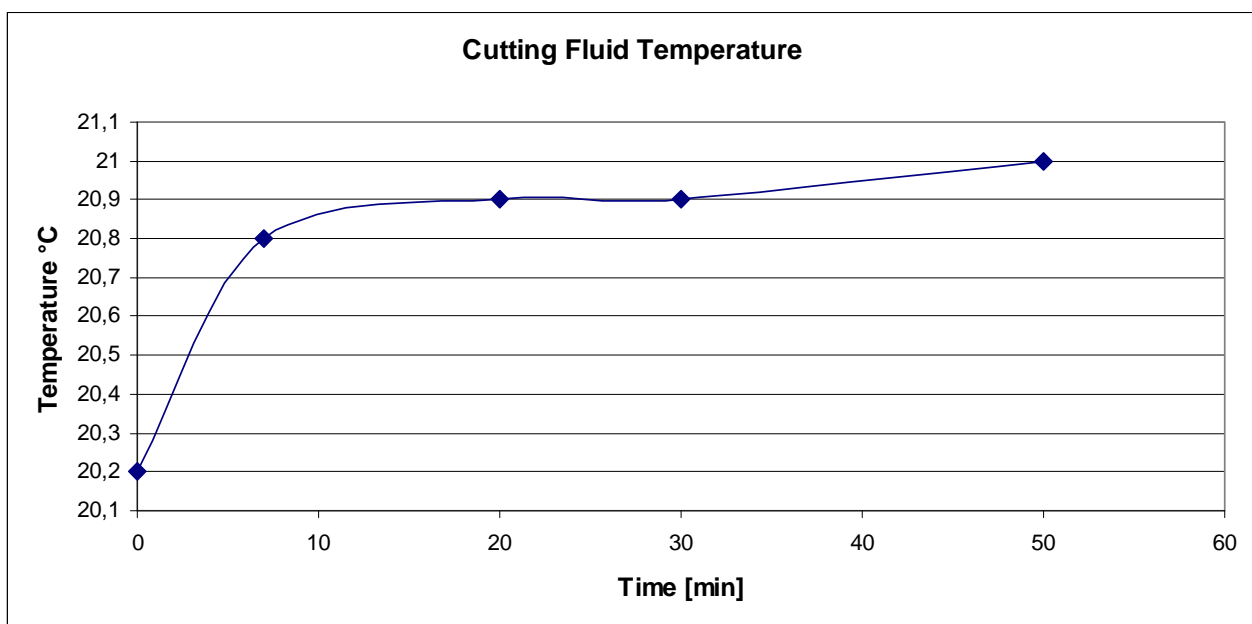Fig. 9 Effect of the cutting fluid on the tool tip position in Z direction.

Fig. 10 Variation of cutting fluid temperature during the test.

As shown by the diagrams, the displacement displayed by the inductive probe was stable at approximately 8.5 μm after 45 minutes while the temperature of the cutting fluid stabilizes already after 20 minutes from its activation. The important results from those diagrams are that the thermal equilibrium concerning the cutting fluid is definitely reached after one hour and that the value of the error contribution to the axial depth of cut caused by the cutting fluid alone is +8.5 μm (here + indicates that the effect of the error is to increase the axial depth of cut). This is explainable by the fact that being the cutting fluid initially colder than the machine column, the fluid subtracts heat from the column which therefore locally reduces its temperature. As a confirmation, the average temperature of the machine tool structure in the area where the table is attached to the column changed from 21.6 °C at the beginning of the tests to 20.1 °C at the end of the tests. The results are a contraction of the column as a consequence of the average temperature reduction and a bending of the column as a consequence of the thermal gradient. Both contraction and bending have the effect of bringing the tool tip closer to the machine table and therefore to increase the axial depth of cut relative to the desired one when the tool length correction is carried out before cutting fluid activation.
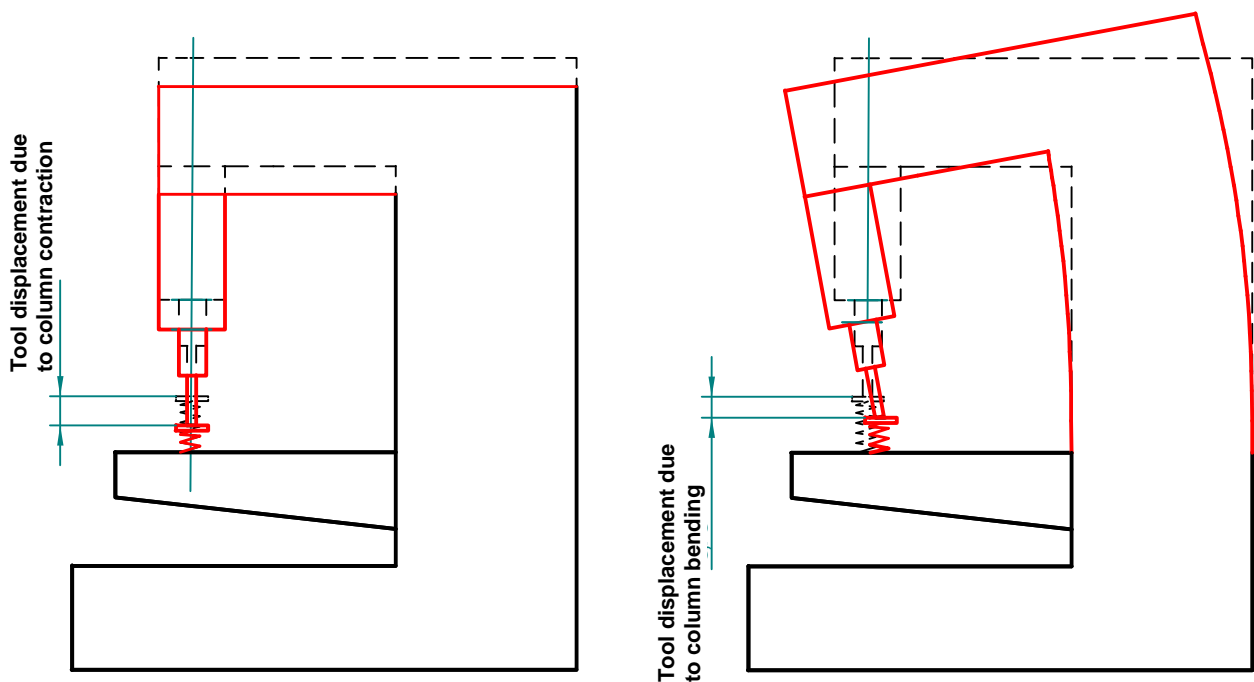

Fig. 11 Variation of tool position induced by the cooling effect of the cutting fluid on the machine column. Left: effect of reduction of average temperature. Right: effect of temperature distribution over the column thickness.

Conclusions

As it became apparent after the test, in order to avoid an error as high as 8.5 μm, the tool length correction had to be performed after the thermal equilibrium between cutting fluid and column was reached (here it should be noticed that machining cycles longer than 2 hours had to be performed and that such a time length was much longer than that required for cutting fluid thermal equilibrium). Unfortunately, the downtime between different operations during which the operator had to work on the machine tool table was quite high, so that such a thermal equilibrium was not guaranteed. Moreover, the cutting fluid was quite aggressive for human skin so that it was not possible to operate on the machine table while the fluid was flowing. Hence a dedicated pipeline was constructed in order to

continuously wet only the machine column without wetting the machine table. In this way it was possible to keep the cutting fluid flowing during the whole working day, even during tool change, tool length correction, specimen replacement and any other operation to be performed with direct contact with the machine tool parts. The flow on the machine table was controlled by a valve which was opened when cutting fluid flow on the table was needed during machining. Figure 12 shows the circuits.

The working procedure was then modified so that during the warm up, the cutting fluid flow was activated and never turned off until the end of the working day, when the machine was shut off. After the warm up, the thermal equilibrium between fluid and column was reached and was assured during any operation by the continuous flowing of the fluid. The only effect still present would be a slight drift of the temperature of the cutting fluid, which would slowly increase its temperature because of the power supplied by the recirculation pump, but its effect on the axial depth of cut was expected to be negligible.
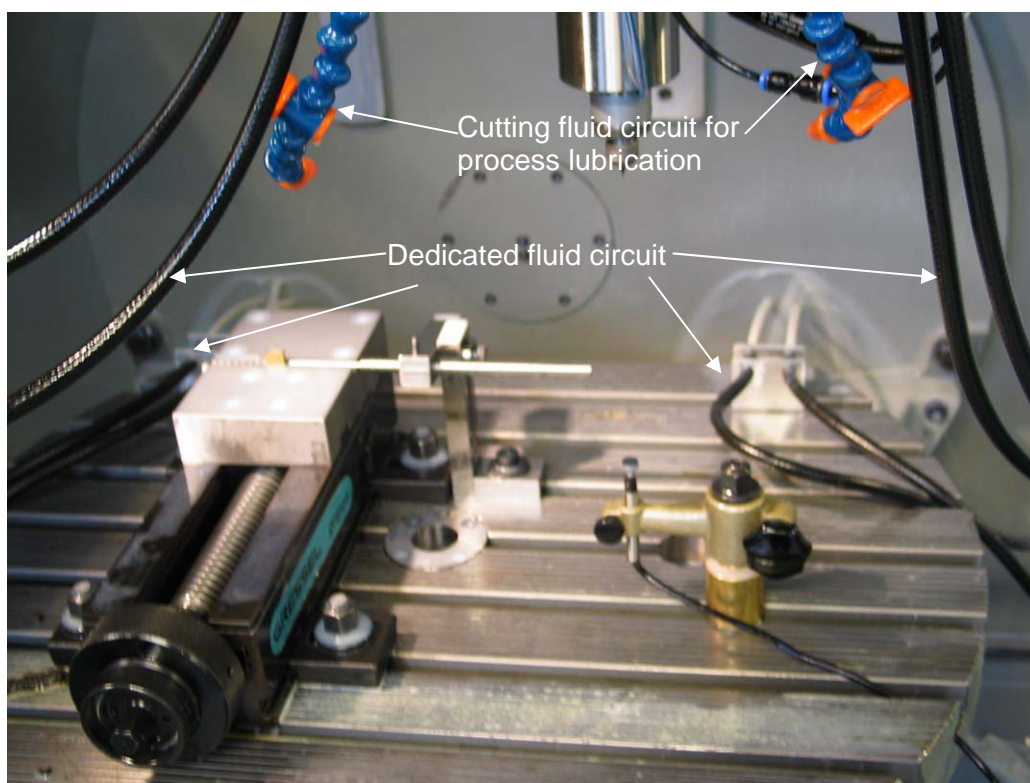
Fig. 12 Modified cutting fluid circuit.

7.2   *Verification of the thermal drift over a period of one hour after compensation for the error due to the cutting fluid*

Verification of the improvement obtained with the additional cutting fluid circuit described above was provided through a dedicated milling test on a brass slab.

Test description

The basic idea of this test was to measure the consistency of the depth of cut, and its agreement with the set value, obtained in a long actual machining operation. Aim of this test was the verification on the workpiece of whether a thermal steady state was actually achieved with the actions discussed above. The test therefore consisted in machining a series of 60 grooves on a brass slab in a period of 1 hour. After machining each groove,

the machine head was kept still for 1 minute and then driven to machine the next groove. The grooves were machined by slot milling using a $\varnothing$ 1 mm flat end mill. The pitch distance between two subsequent grooves was 1.5 mm and the depth was 50 μm. During the waiting time the tool was maintained at the same rotational speed as for the machining phases. Moreover, in order to avoid the effect of the repeatability of positioning on the observed depth of cut, the CNC program as obtained from the CAM was modified so that in the whole program, only 1 command for movement in Z direction to the required depth was given. The reference surface for the measurement of the depth of cut was produced by a milling operation using a $\varnothing$ 6 mm flat end mill. The details of the machining sequence are as follows:

Roughing :   Tool: OSG FXS-EMSS $\varnothing$6 mm, 6 flutes
                     f = 500 mm/min
                     n = 13000 rpm

Slotting: Tool: OSG WX-LN-EDS $\varnothing$1 mm, 2 flutes
                     f = 100 mm/min
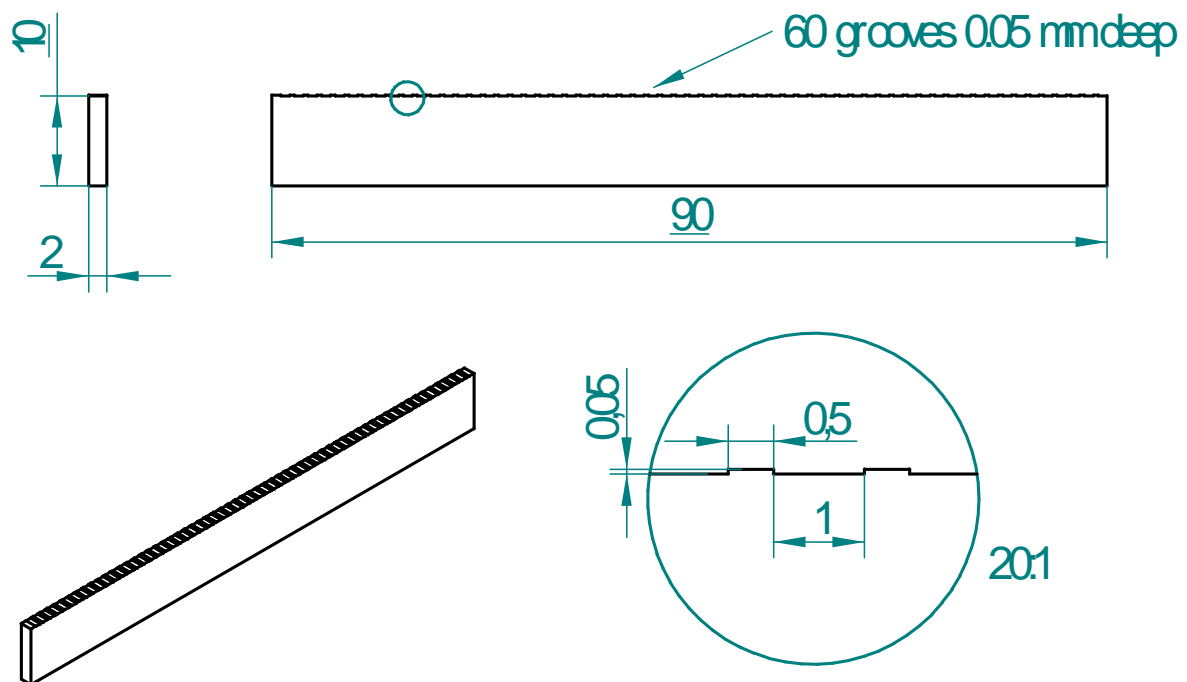   n = 15000 rpm

Fig. 13 Sketch of the specimen for verification of depth of cut control.

The temperature of the cutting fluid was also monitored during the machining operation.

Results
Measurements of the depth of the grooves was carried out using a contact profilometer Taylor-Hobson RTH Talysurf 5-120 with Z resolution of 0.001 μm and the evaluation was based on the standard ISO 5436. The diagram in fig. 14 shows the results.
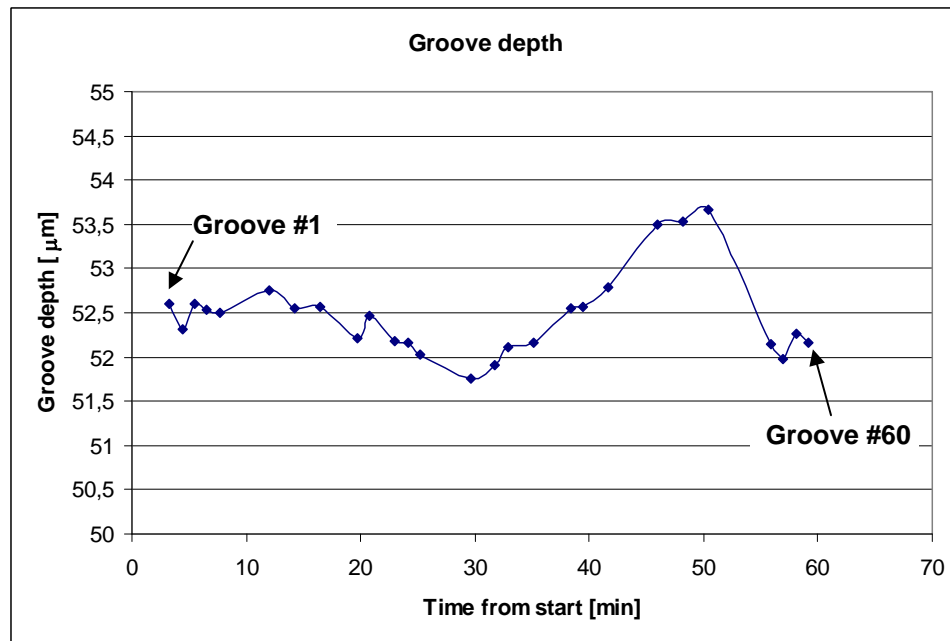
Fig. 14 Measured depth of the machined grooves.

From fig. 14 it appears that the actual depth of cut was approximately 52.7 μm $\pm$1 μm with a maximum deviation from the nominal one of +3.7 μm. This constitutes an improvement in comparison to the initial situation, since the deviation is definitely smaller than the 8.5 μm due only to the effect of the cutting fluid. During the machining operation the temperature of the cutting fluid increased of only 0.1 °C. However, the tool length correction required after the warm up cycle with flowing cutting fluid was 14 μm.

Observation of the profile of the test workpiece highlighted that the top and the bottom of the machined grooves were arranged along two identical curved lines. Since the slab was aligned with the machine tool X axis, this clearly means that a curvature of the machine tool slideways in X direction was present. The detectable straightness error was 5 μm over a length of 90 mm.
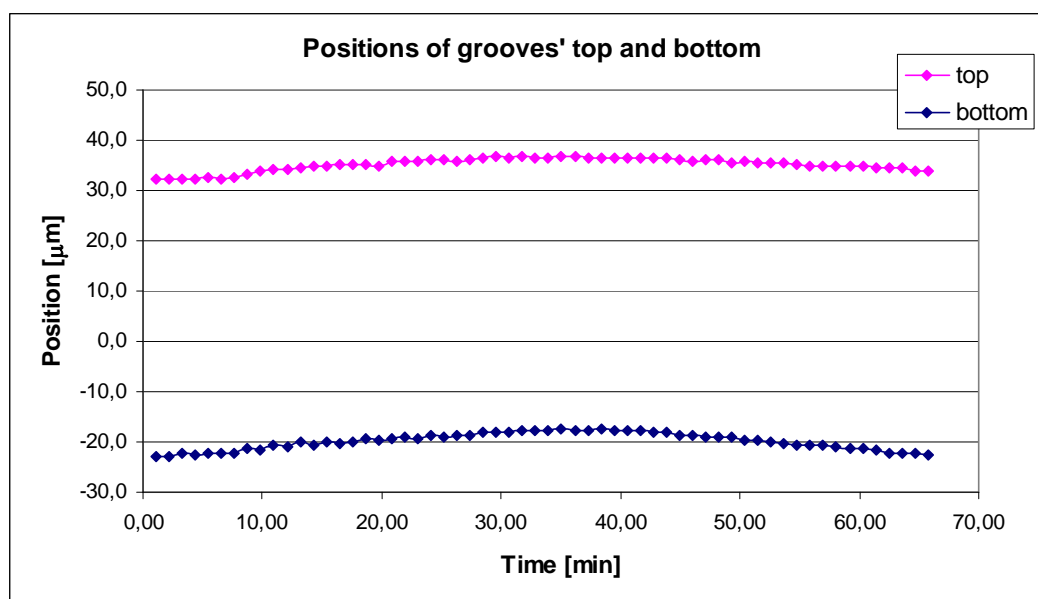

Fig. 15 Top and bottom of the grooves are arranged on two identical curvilinear profiles. The interpretation is a straightness error of the X axis slideways of 5 μm.

Conclusions

Apart for the revelation of the straightness error of the machine slideways, this test proved the improvement in the control of the depth of cut even though an error of almost +4 μm was still present. This residual error was explained as a possible misalignment between the spindle axis and the normal to the surface of the inductive probe in connection with the use of tools of different diameter, according to what discussed in paragraph 5.4 and shown in fig. 8. With the diameters used in this test (6 mm and 1 mm) the angle necessary to produce an error of +4 μm would be approximately 0.1°. Therefore a test was defined to check for this possible misalignment and will be presented in the next paragraph.

The fact that after the warm up the correction of the tool length required was 14 μm instead than 8-9 μm was attributed to the substantial difference that during the warm up phase the machine tool has been moving for 1 hour, therefore warming up by friction the slideways as well, while during the test described in the previous paragraph the effect of the cutting fluid alone was considered and isolated.

7.3   Identification of misalignment error of inductive probe's tip

A further analysis of the working procedure has highlighted the possibility of positive errors (referring here to the direction of the error towards an increase of the depth of cut) of the axial depth of cut induced by misalignment between the inductive probe axis and spindle axis. This has been verified by scanning the surface of the tip of the inductive sensor with a plug inserted in the high speed spindle having a spherical end.

Test description

The basic idea was to scan the flat tip of the inductive sensor with something that could move in X and Y directions at a constant Z height having the inductive sensor itself displaying its misalignment. In order to carry out the test, a cylindrical pin with an internal thread was manufactured. A spherical tip, normally used for dial gauges, was screwed in the internal thread and the pin was mounted in the chuck of the high speed spindle. With the pin positioned in the zero position in X and Y, in the reference system G57 used for the tool length correction, which corresponds to the centre of the flat tip of the inductive sensor, the machine head was lowered until the zero point of the inductive probe was reached. Then repeated scans on the flat tip in X and Y direction were taken, with point interval of 500 μm. Before the scanning, the updated warm up procedure (the one with cutting fluid on) was applied so that thermal stabilization was reached. Both the spherical and the flat tips have been accurately cleaned before the test. For each point in the scanning path, a time of 20 seconds was allowed for stabilization of the detected value.

Results

Five scans were taken in both directions and the average diagrams are shown in fig. 16 and 17.
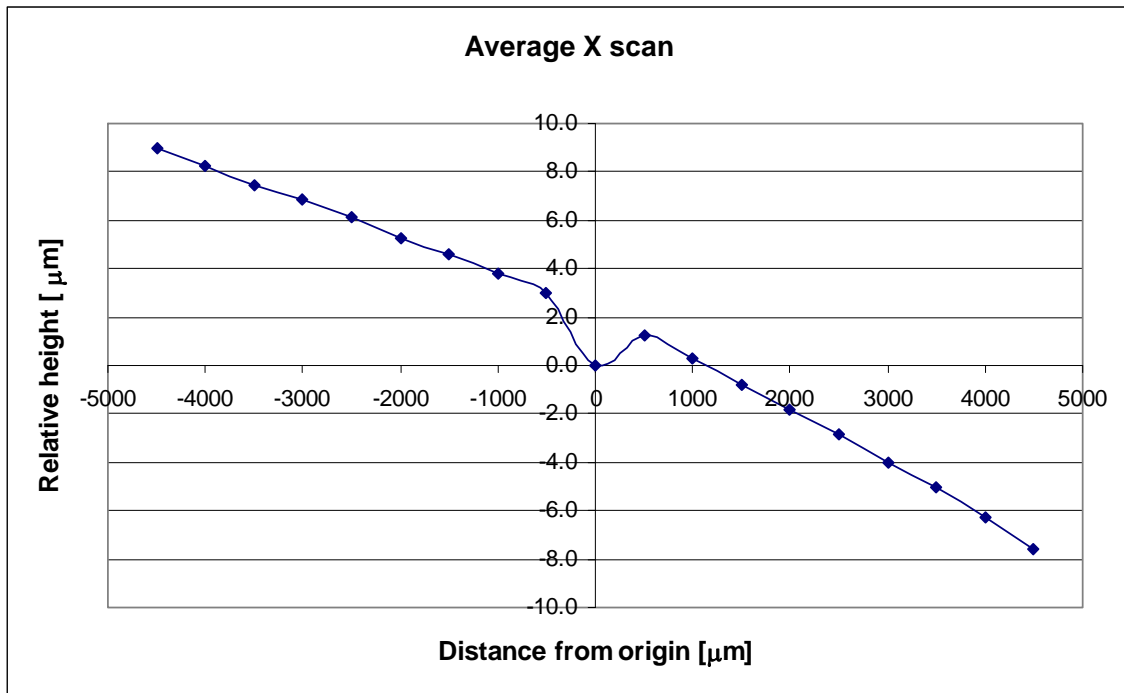
Average X scan

Fig 16 Profile of the tip of the inductive probe in X direction. Average of 5 repeated scans.
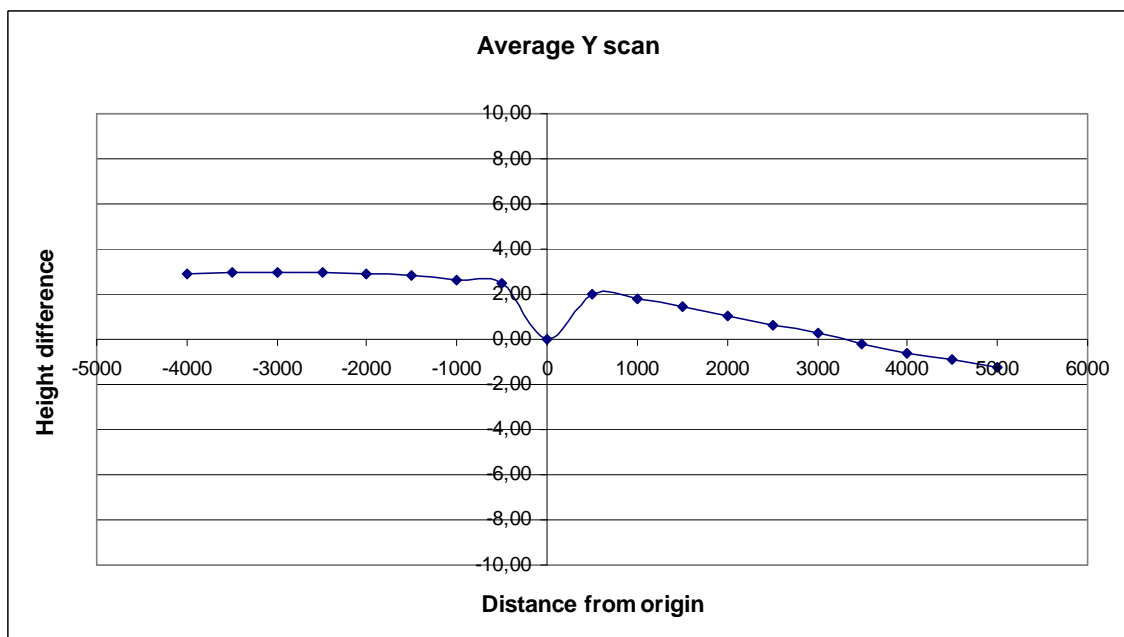
Average Y scan

Fig 17 Profile of the tip of the inductive probe in Y direction. Average of 5 repeated scans.

As suspected the diagrams show a clear tilt of the flat tip in both direction with the tilt in X 3 times bigger than that in Y. Moreover, a scratch is present in the centre of the tip, which further increases the error when very small tools ($\varnothing$ 0.2 mm) are used to generate the functional surfaces. Combining the two directions <u>the total inclination angle</u> (calculated through the sum of square of the angular coefficients in the X and Y directions) <u>is</u> **0.107°** which is even more than what was expected.

The resolution of the scans was too low to allow proper characterization of the scratch in the centre of the flat tip. The scratch was therefore further investigated with two more scans in X and Y direction, limited to the central area of the tip, using a point interval of

100 μm. As shown in fig. 18 and 19, the scratch resulted to have a dimension of 300 μm in both directions.
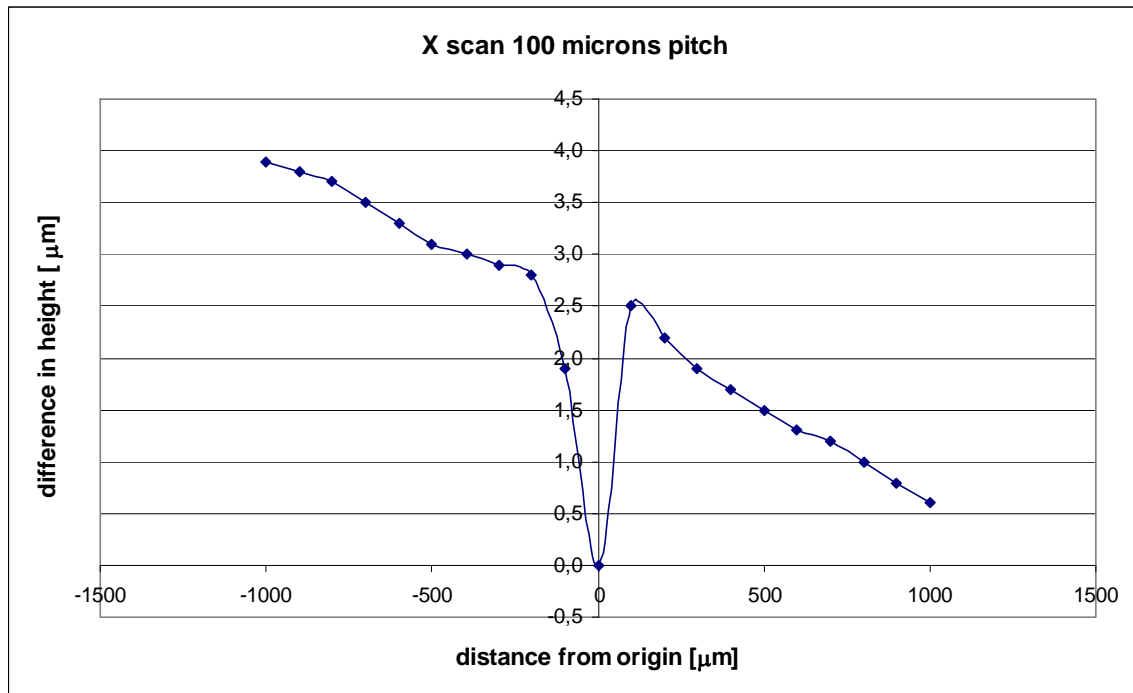

Fig. 18 Profile of the tip of the inductive probe in X direction with point interval of 100 microns.
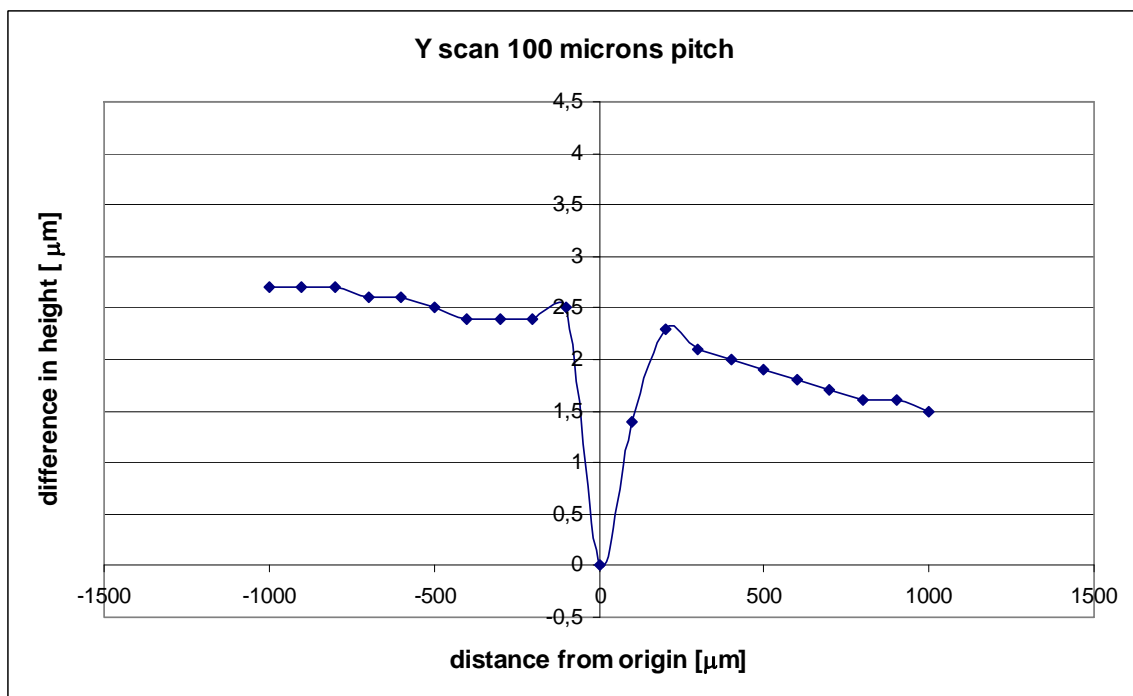
Fig. 18 Profile of the tip of the inductive probe in Y direction with point interval of 100 microns.

Conclusions
The knowledge of the inclination angle of the flat tip of the inductive probe and of the two diameters used for generating reference surfaces and functional ones, allows either compensation for the related axial depth of cut error or its avoidance. In any of the cases, contact of the tools with the central area of the tip, where the scratch is present, must be

avoided. This is mandatory for the small diameter end mills that can completely fall into the scratch, while for large flat end mills (i.e. ∅ 6 mm), this does not constitute a problem because of the concavity of the bottom of the end mills. For the larger end mills contact will always occur at the periphery and therefore outside the scratch. The first action is then to use X and Y positions for the tool length correction far enough from the central scratch. Therefore the position X= − 1.2 mm Y=0 in the G57 reference system was chosen (the angle between X and the direction of the gradient of the surface of the flat tip was 15°, thus the influence of the tip inclination in Y direction was neglected). Negative direction was chosen for the X displacement because the slope of the surface of the flat tip in X direction is negative.

At this point, <u>compensation</u> for the axial depth of cut error could be obtained through calculation of the expected error and by correction of the tool length in the machine control:

$$\Delta l = \frac{D_1 - D_2}{2} \tan\alpha \qquad\qquad (1)$$

where D_1 and D_2 are the tool diameters, α is the inclination angle equal to 0.107° and Δl is the tool length error.

<u>Avoidance</u> of the error is instead possible if the points where contact between tool and flat tip occurs are the same for the two end mills. Since the slope of the surface of the flat tip in X direction is negative, this is obtained if the tool length correction for the smaller tool is performed at a position shifted of $(D_1-D_2)/2$ in the negative X direction.
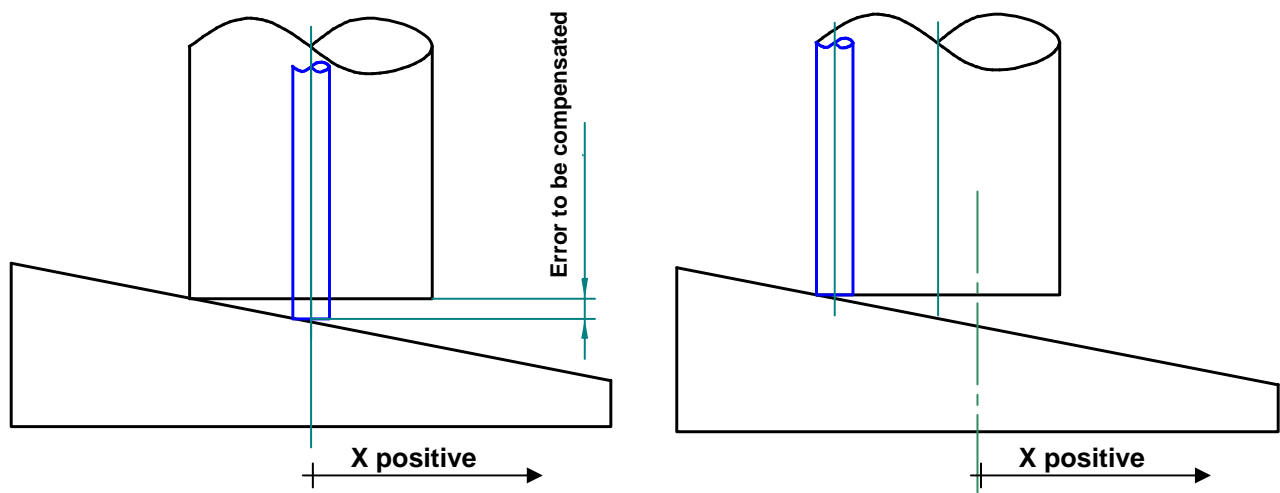

Fig. 19 Ideal sketch of the two solutions for the misalignment of the tip of the inductive probe: left, compensation; right, avoidance.

It should be noticed here that the problem connected with the inclination of the flat tip surface does not exist when the tools used are all ball nose end mills, because the contact point is practically the same even though the diameters are quite different. It is easy to demonstrate in fact, that, for two ball nose end mills having diameters of 0.2 mm and 6 mm, the error in tool length introduced by neglecting the tip inclination is 5 nm.

In order to prove the benefit of the compensation for the contribution to the axial depth of cut error described in this paragraph, a new test on a brass slab identical to the one reported in par. 7.2 was carried out. Such a test is presented in the next paragraph.

7.4   *Verification of the axial depth of cut error over a period of 1 hour after correction for the misalignment between tool axis and inductive probe*

For this test, the conditions, tool diameters, workpiece material, rotational speeds ecc. were identical to those reported in 7.2, the only difference was the correction introduced to compensate for the inclination of the flat tip of the inductive sensor. Among the two solutions presented above, the chosen one was the compensation. With the two diameters used and the calculated inclination angle, formula (1) gives a correction Δl = 4.67 μm. Thus the depth of cut of the single pass for generation of the reference surface (previously called roughing) was intentionally increased of 5 μm (the resolution of the parameters set in CNC programs and in the machine control was 1 μm).

Results

Measurements of the depth of the grooves was carried out using a contact profilometer Taylor-Hobson RTH Talysurf 5-120 with Z resolution of 0.001 μm and the evaluation was based on the standard ISO 5436. The diagram in fig. 20 shows the results.
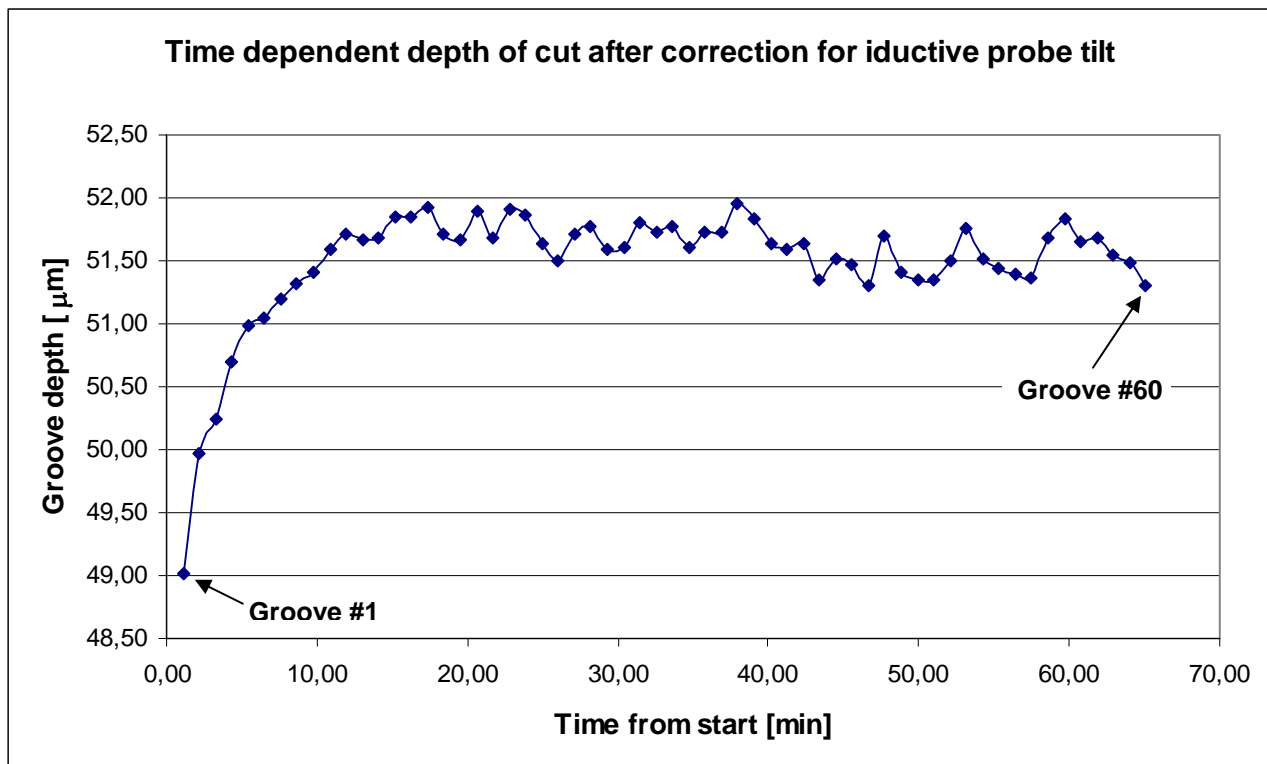

Fig. 20 Measured depth of the machined grooves.

From the analysis of the diagram it appears that the axial depth of cut was stable at a value around 51.5 μm but only after approximately 40 minutes. However the most apparent thing is that the machine tool is not thermally stabilized yet and the axial depth of cut varies from about 49 μm at the beginning of the operation to 52 μm after 18 minutes.

Conclusions

As it will be shown later this effect was due to the elongation of the high speed spindle due to thermal expansion. However the range of variation of the depth of cut appeared to be included in ± 2 μm which was considered to be good enough for the experiments to be carried out. Nevertheless tentative machining with $\varnothing$ 0.2 mm ball nose end mills still

resulted in systematic breakage. According to the knowledge of the process available at the moment, it was doubted whether or not the tools could withstand to the cutting forces corresponding to the chip load, defined in the experimental plan, for the machining of the hardened tool steel. Therefore a dedicated test was performed to verify it.

7.5   First test workpiece in Elmax for verification of the ability of the 0.2 mm tool to withstand an axial depth of cut of 10 μm.

This machining test was designed to clarify whether or not the reason for systematic breakage of the 0.2 mm end mills was that the tools were unable to withstand to the nominal load, corresponding to a depth of cut of 10 μm. Because of the purpose of the test, the workpiece material, the tool (obviously) and the cutting data were the same as those used in the machining experiments to be carried out afterwards.

Test description

The geometry of the workpiece consisted of a series of steps generated on hardened tool steel by means of parallel passes with the 0.2 mm ball nose end mill. The tool passes were taken at Z levels from +30 μm to -15 μm from the flat surface generated with a $\varnothing$ 6 mm flat end mill. The incremental depth was 5 μm. The sketch in fig. 21 illustrates the situation.
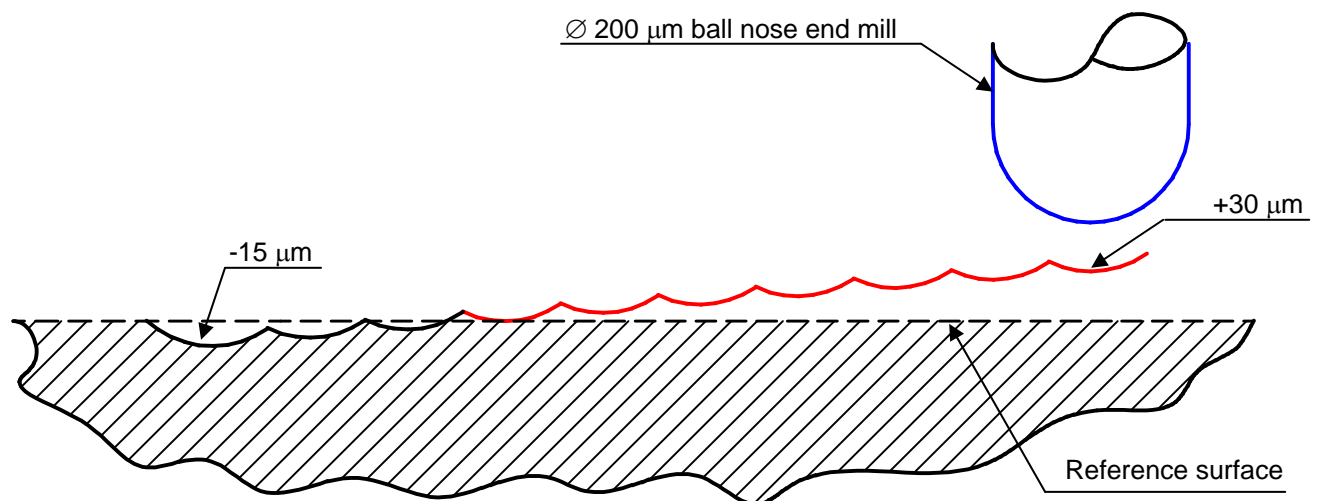

Fig. 21 Sketch representing the layout of the surfaces to be generated during the test.

The parallel passes followed one another from right to left, and in case of good accuracy, only the last three passes should have engaged the material. Since the depth of cut set in the ball nose end milling experiments to be carried out was 10 μm, the specimen was designed in a way to check what happened also with depths of cut ±50% from the ideal one. The pattern was repeated twice in rapid succession with the same tool, shifted in X direction of a convenient distance. The details of the machining sequence are as follows:

Generation of reference surface :   Tool: flat end mill OSG FXS-EMSS $\varnothing$6 mm, 6 flutes
                                           f = 100 mm/min
                                           n = 6350 rpm

Generation of the steps: Tool: ball nose end mill OSG WX-LN-EBD R0.1 x 0.5, 2
                                 flutes
                                 f = 63.66 mm/min
                                 n = 31831 rpm

The position for the tool length correction of the ∅6 mm flat end mill was X=0 Y=0 in the reference system G57 and, avoidance of the misalignment problem was obtained performing the tool length correction of the ball nose end mill at location X= -3.0 Y=0, which is the contact point between the flat end mill and the flat tip of the inductive probe (here notice that the second end mill is a ball nose and its contact point is practically coincides with its axis). The tool could machine both the patterns without breakage. Again measurements of the generated surface was carried out using a contact profilometer Taylor-Hobson RTH Talysurf 5-120 and a representative profile for the two patterns is shown in fig. 22.
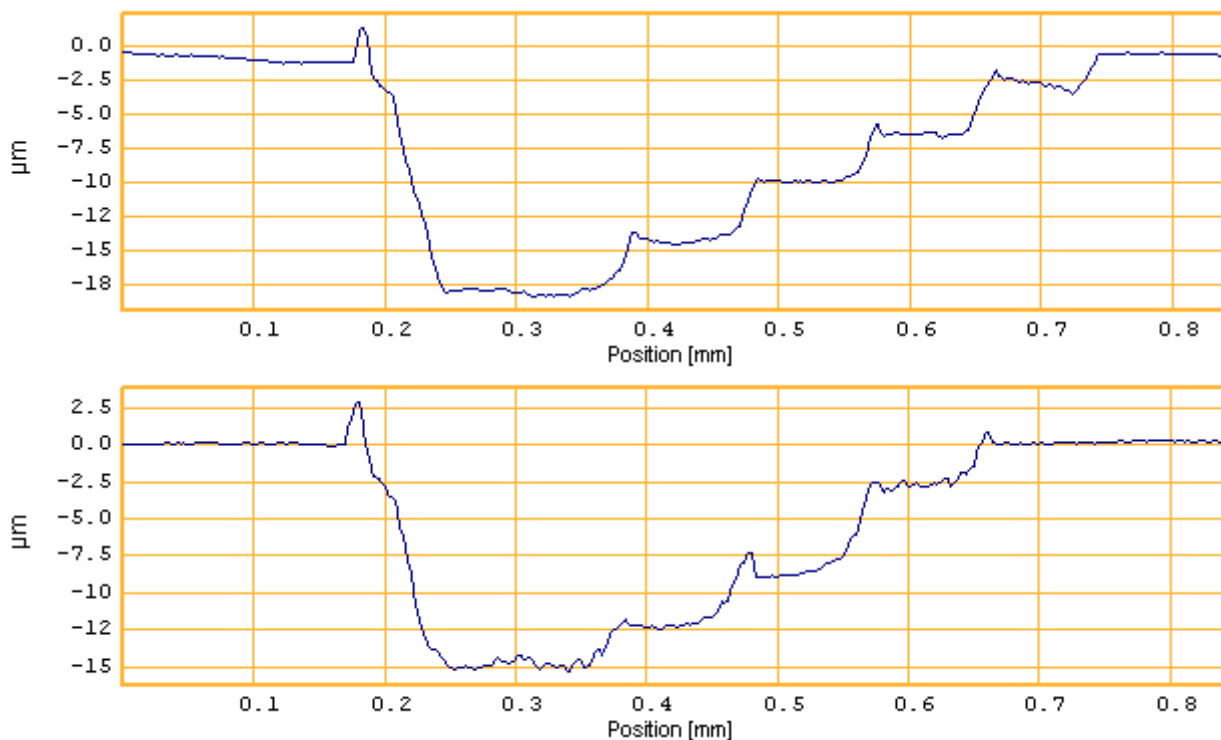

Fig. 22 Representative profile of the machined patterns. Top: first series of steps. Bottom: second series of steps.

Results
The results were rather bad as concerns the depth of cut accuracy. In fact in the first pattern 5 passes have engaged the material (2 more than desired), with a maximum error of 8.4 μm in the first step which was supposed not to be engaged (+5 μm above the surface). In the second pattern 4 passes have engaged the material (1 more than desired) and the maximum error was reduced to 3.9 μm. Due to the high error, the maximum depth of cut was 18.3 μm. This proves the tool could withstand to the design load corresponding to 10 μm of axial depth of cut, which was the main objective of the test. Besides this, the elevated maximum error showed that, apparently, something was still out of control. An accurate observation of the measured profiles highlighted the character of constantly decreasing magnitude of the depth of cut error while the machining proceeded. This is shown in fig. 23.
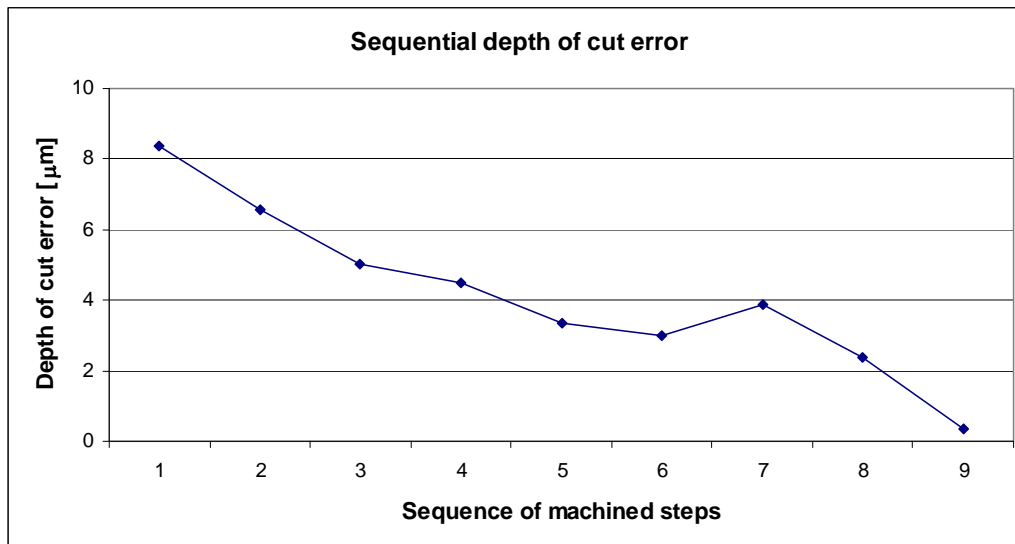
Sequential depth of cut error

Fig. 23 Variation of the depth of cut error with the proceeding of the machining operation in the present test.

The difference between the initial and the final error is 8 μm. This is clearly the effect of tool wear, particularly severe because the tool is cutting with its centre, where the cutting speed is zero. Just after the machining, the tool length was checked again to verify the influence of wear and the reliability of its control with the improved procedure, showing a tool length 7 μm shorter than the initial one. This is in good agreement with the maximum error difference showed in fig. 23. Moreover, the rotational speed used for this test was much higher than that for the previous tests and corresponded to that used for some of the unsuccessful trial experiments. Putting all this things together, a possible explanation was that the attached spindle unit, rotating at high speed, was generating much higher heat power than in the previous tests and, therefore, slightly increased its length. At the end of the machining operation, the spindle had time enough to partially cool down, and at the moment of the tool length correction after machining, the 7 μm of length reduction resulting (-7 μm) were the combination of the 8 μm coming from the tool wear (-8 μm) and 1 μm due to the residual spindle thermal expansion (+1 μm). In view of these considerations, a much higher thermal expansion of the spindle had to be expected, since it had some time to cool down before the check.

Conclusions
Despite the bad result, this test was very helpful for a better understanding of the phenomena involved in the process and gave some hints for further optimization. Summarizing what described above, this test has shown that:

- the tool could withstand the load corresponding to the design axial depth of cut with the material in use;

- extremely high tool wear is present when milling hardened tool steel with the ball nose at 0° inclination angle;

- Increasing the rotational speed a noticeable thermal expansion of the high speed spindle, which was not detected in the other tests, occurs with small time constant.

In order to improve the control on the axial depth of cut it was therefore decided to investigate the thermal behaviour of the high speed spindle which is the subject of the next paragraph.

7.6   Identification of the high speed spindle thermal drift, calibration of its expansion for different speeds and development of a compensation procedure

A preliminary investigation of the thermal behaviour of the high speed spindle has been carried out first, concerning the temperature reached in the most significant point in different conditions. This has shown that spindle expansion was not negligible. Further test have shown that, in certain conditions, spindle expansion was an outstanding factor in contributing to the total axial depth of cut error. Reckoning that an optimum control was necessary only with the rotational speeds to be used in the experiments, a calibration of the spindle expansion in Z direction at specified rotational speeds was carried out and calibration curves were obtained.

Test description

At this point several machining trials had been run with slight variations in the procedure. It was tried also to warm up the spindle for several minutes just before the tool length correction so that spindle elongation was supposed to be present at the moment of tool length correction, but the improvements obtained were not sufficient for the successful machining using ball nose micro end mills. The experience gained so far anyways led to consider whether the spindle thermal behaviour was characterized by a small time constant, such that the time required for tool change and tool length correction was long enough to reduce the spindle temperature and, therefore, the spindle length, of an amount that could produce a considerable error on the estimation of the tool length in working conditions. As described above, the attached spindle was driven by a high frequency brushless motor directly connected to the spindle and mounted on top of it. The motor was cooled by air flow at pressure variable between 2 and 6 bar and a device protection circuit prevents the spindle to start if the air pressure is too low. Since the air flow starts when the spindle control unit is turned on and continues even during the downtimes, when the spindle is stopped, it was considered whether the closure of the air circuit when the spindle was stopped for tool length correction was effective on slowing down the spindle cooling.

A dedicated test was thus carried out, consisting in continuous monitoring the spindle temperature during warm up at a defined rotational speed (active phase) and during the subsequent cooling (passive phase) as well. The test was repeated twice, once with the cooling air always active and once with the cooling air turned off at the moment of spindle stop. In order to carry out the test, a single point thermocouple was used (type….) and the most significant point was found to be located at the end of the spindle casing, close to the rotating part. In fact, this was a constriction since it was the only accessible place were the casing was not covered by the thick spindle holder. In that place the measured temperature variations were higher and therefore the relative measuring uncertainty was lower. The rotational speed chosen for the test was 30000 rpm; the duration of both the active phase and the passive phase was 10 minutes and the room temperature was 21.6 °C for both the test runs. The diagram in fig. 24 shows the results.
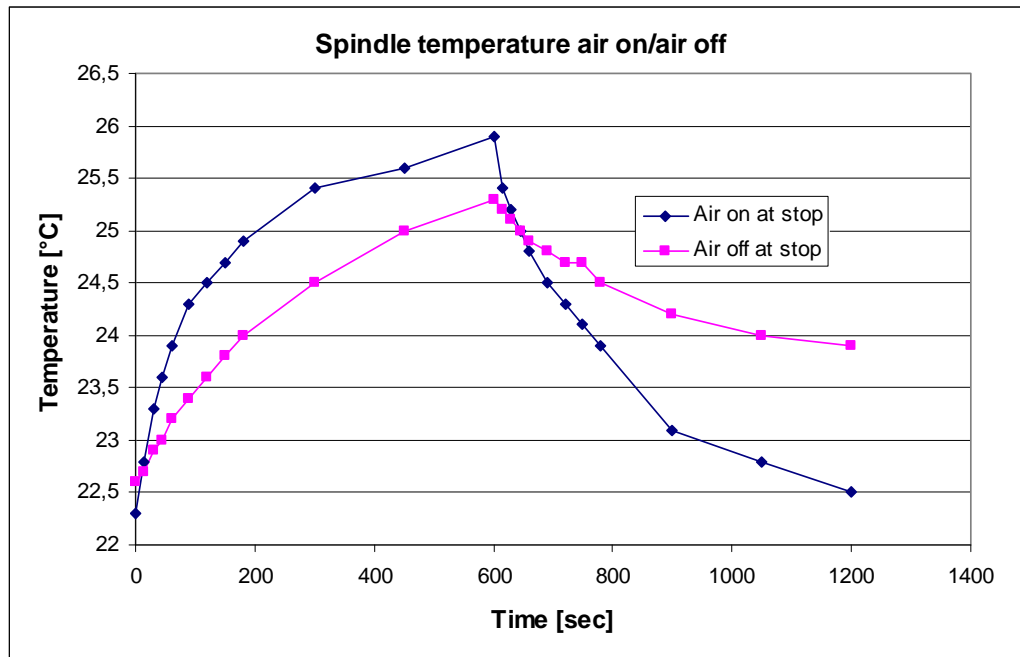
Fig. 24 Comparison between spindle temperature during warm up at 30000 rpm and subsequent cooling with air on and air off at spindle stop. Room temperature for both tests 21.6 °C.

Although the maximum temperature reached by the spindle was not the same (this can be due to the variation of the cooling air temperature, that in turn depends on which of the two compressors of the air supply system is running at that moment), it is apparent that for the same temperature range, the slope of the curve during the cooling phase is much lower when the air is closed at stop. However, the temperature variation at 30000 rpm is more than 4.5 °C after only 10 minutes rotation which does not constitute the steady state temperature as is apparent from the slope of the last part of the ascending curves. Further investigation were therefore carried out in order to check for the influence of the rotational speed and it was found that the maximum temperature, reached in a specified time length, was highly dependent on the spindle speed. Particularly, a test was made to determine the spindle temperature increase, at steady state, for the 4 rotational speeds to be used in the experiments. As can be seen in fig. 25, which displays the difference between spindle temperature and room temperature from start to steady state, for rotational speeds below 16000 rpm, temperature increase is small and the influence of the rotational speed is negligible. However, at increasing speeds, the temperature rise is noticeable and is highly affected by the rotational speed. Furthermore the time required for reaching the steady state increases with rotational speed.
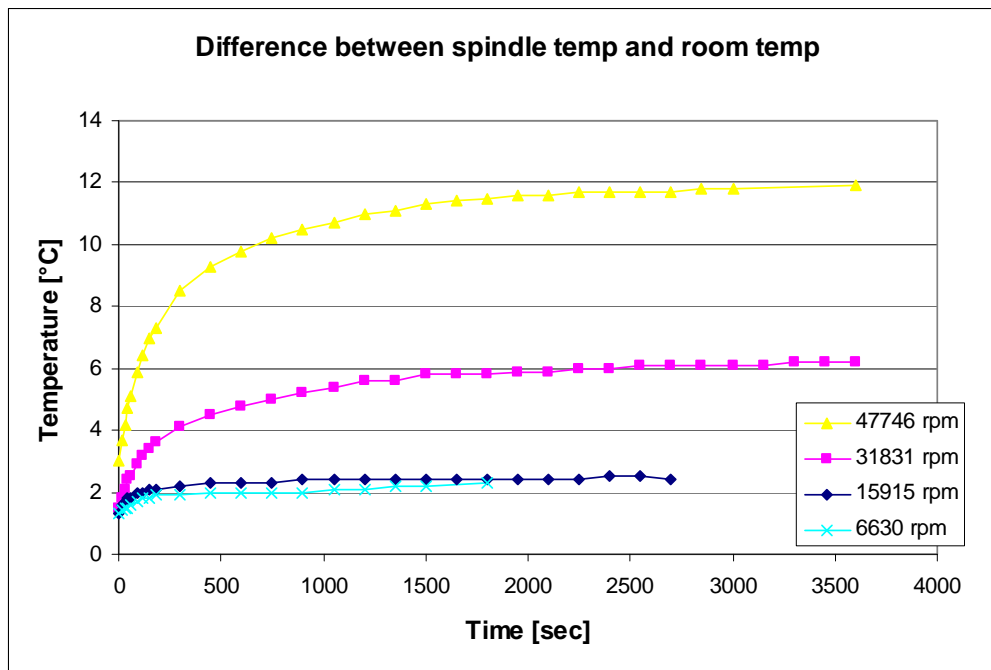
Fig. 25 Spindle steady state temperature at different rotational speeds.

In order to reach a better control of the axial depth of cut, a solution was therefore to carry out a calibration of the spindle expansion for the rotational speeds to be used in the experiments. In this way, by recording the spindle temperature when the tool length correction was performed, and knowing the temperature the spindle was going to reach at its steady thermal state, estimation of the expected spindle length increase was possible and the tool length could be further corrected in the machine control. Then warming up the spindle before engaging the workpiece, until the expected working temperature was reached, the actual tool tip axial (Z) level should be the one corresponding to the tool length stored in the machine tool control and the spindle temperature should not further increase and no further elongation of the spindle have to be expected. Here it should be noticed that although a single point temperature cannot be representative of the whole machine tool temperature distribution, if the same border conditions (read operating conditions) are created, the same effects have to be expected. Thus, the temperature distribution in the machine tool should be the same and eventually the machine tool and spindle deformations. In other words, it is expected that the machine tool behaviour is repeatable. This is the reason for the choice of the rotational speeds for the calibration. In fact being exactly the same as the ones used in the experiments, one of the requirements for recreating the same operating conditions is fulfilled.

The mentioned calibration was carried out by warming up the spindle to its thermal steady state and then quickly moving the tool tip to the tool length correction position on the inductive probe. The reading of the inductive probe and the thermometer display were recorded at regular intervals for a period of time sufficient to display a temperature and length variation rate reasonably small. By plotting the length variation versus the measured temperature, a curve for each spindle speed is obtained (fig. 26). The angular coefficient of the lines obtained by linear approximation of the data points, can then be used for the calculation of the length increase expected in the working conditions, once the temperature of the spindle, at the moment the tool length correction is performed, and the steady state temperature are known.
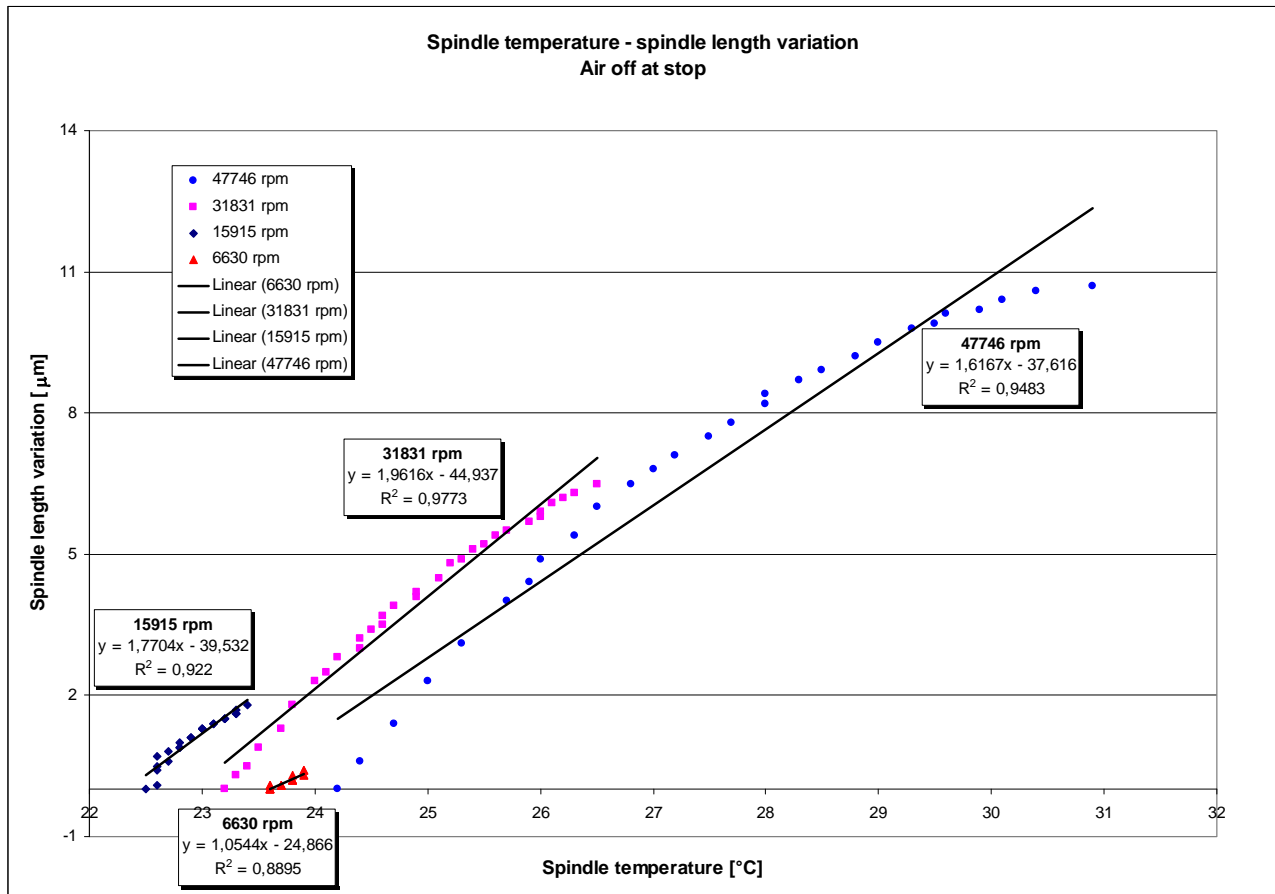
Fig. 26   Spindle temperature-spindle length calibration curves for the 4 rotational speeds to be used in the machining experiments.

As is apparent the four point distributions would be better approximated by a second order polynomial. However, a more complicated approximation formula than the linear one would introduce further difficulties for the machine tool operator since the slope of the curve must be calculated for correction of the tool length value stored in the CNC control. This correction has to be added to the one performed on the inductive probe. The correction value is calculated according to the following formula:

$$\Delta l = m \ \Delta T \tag{2}$$

Where Δl is the elongation of the spindle to be expected for the difference ΔT between the steady state spindle temperature, for the relevant rotational speed, and the spindle temperature at the moment of the tool length correction. m is the slope of the approximating line for the relevant rotational speed. The value Δl must be added to the tool length value stored in the CNC control after the normal tool length correction has been performed.

 With the obtained calibration curves, the working procedure changes to the following:

1. Machine warm up for 1 hour, with coolant on, at a rotational speed of 30000 rpm using a machining program originally created for a roughing procedure and repeated several times.

2. Tool length correction (from now on called tlc) on the inductive probe with the $\varnothing$ 6 mm ball nose end mill (roughing tool) away from the probe tip centre.

3. Spindle warm up with the rotational speed used for the roughing.

4. Reading of the spindle stable temperature at the steady state.

5. Tlc with the rouging tool in the same position as point 2, with the cooling air of the spindle turned off, and reading the spindle temperature at the moment of the correction.

6. Further correction of the tool length for the temperature difference between point 4 and 5.

7. Spindle warm up, with rotational speed used for roughing, to the temperature found in point 4.

8. Performing the roughing and recording the maximum spindle temperature reached.

9. Changing the tool to the finishing end mill and spindle warm up with the rotational speed required for the relevant cutting data set.

10. Reading of the spindle stable temperature at the steady state.

11. Tlc with the finishing tool in the same contact point as for the roughing tool (point 2), with the cooling air of the spindle turned off, and reading of the spindle temperature at the moment of the correction.

12. Further correction of the tool length for the temperature difference between point 10 and 11.

13. Spindle warm up, with rotational speed used for finishing, to the temperature found in point 10.

14. Performing the finishing and recording the maximum spindle temperature reached.

15. Repositioning the tool in the tool length correction position and recording of temperature and length variation over a short period of time.

16. Extrapolation of the tool length at the working temperature and calculation of the total tool wear at the tool tip.

The calibration curves are used in point 6 and 12 of the described procedure.

In order to prove the reliability of the method and the improvement introduced by the use of the calibration curves, some test specimens, with a particular design for control of the accuracy of the depth of cut, have been machined and measured. The following paragraphs report the results.

7.7   *Second test workpiece in Elmax for verification of the improvement obtained by use of the calibration curves.*
Aim of this test was to check for the total accuracy of control of the axial depth of cut, with the improved procedure, in exactly the same conditions as for the actual machining experiments to be carried out afterwards. The workpiece material, the tool type and diameter, the cutting data were the same as for the test described in paragraph 7.5. The pattern described there was machined only once in the present test. The scope of the test constitutes the main difference.

Test description
For a detailed description of the test, see par. 7.5.

Results

Measurements, as usual were carried out using a contact profilometer Taylor-Hobson RTH Talysurf 5-120. Two areas of the specimen surface, one in the centre and one on the side of the machined area, were scanned and 10 profiles on each one have been evaluated. Fig. 27 displays a representative profile.
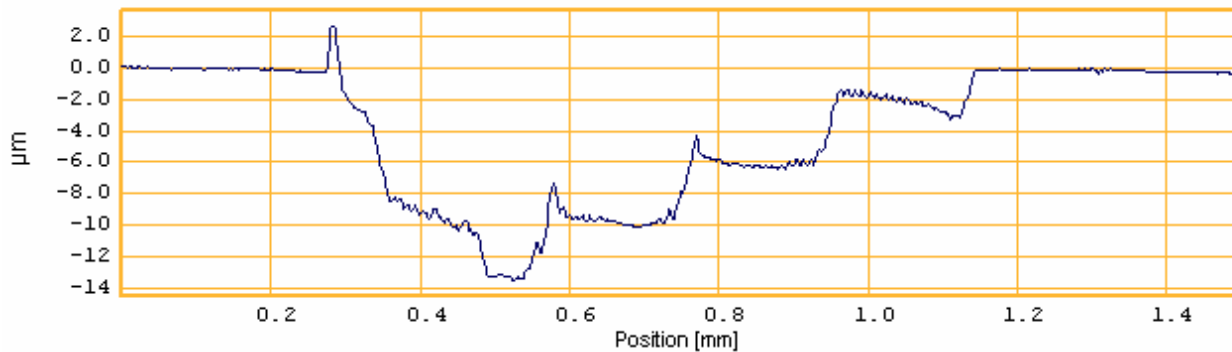

Fig. 27 Representative profile of the machined pattern.

The average results showed that the control has improved substantially in comparison to the previous test in par. 7.5. The first 4 passes have engaged the material (one more than desired) and the maximum error was 2.07 μm. Unlike the previous test, where the initial error on the depth of cut was more than 8 μm and was reduced only by effect of the tool wear, here the initial depth of cut error on the first step (therefore unaffected by tool wear) was +2.07 μm (+ indicates deeper than desired) and changed to -1.95 μm on the last step at the end of the machining cycle. Again the effect of the tool wear is apparent, as displayed in fig. 28.
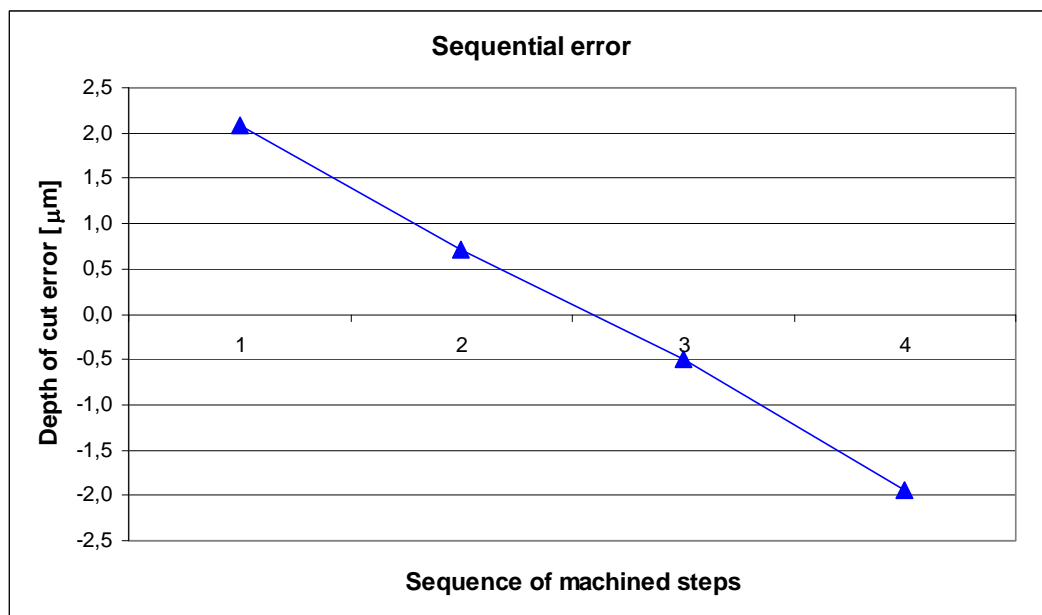

Fig. 28 Variation of the depth of cut error with the proceeding of the machining operation in the present test.

A noticeable fact is that the slope of the sequential error curve is constant and quite comparable with that of the previous similar test, being the width of the workpiece the same.

Conclusions

The improvement introduced with the calibration curves is apparent. Considering only the first machined step, where tool wear is not manifest yet, the error is close to 2 μm. However, the workpiece material was very hard and high tool wear rate was present. Moreover, the shape of the mill and therefore the generated profile, was not optimal for accurate measurement of the axial depth of cut and the step depth of the pattern was 5 μm (which too coarse for very fine depth of cut adjustment). Finally, the amount of material the tool engaged was never the same on the two sides, thus introducing possible lateral deflections of the tool. A test unaffected by tool wear and more suited for precise measurements was needed. A better prove of the accuracy of control of the axial depth of cut would be provided by slot milling on a softer material using a flat micro end mill with a smaller incremental depth.

7.8   First test workpiece in brass for verification of the achieved depth of cut accuracy without tool wear effects.

Objective of this test was the verification of the overall improvement introduced with all the modification, to the initial procedure, resulting from the previous tests. Unlike the previous one, in this test brass was used as workpiece material in order to minimize the effect of the tool wear on the measurements. Moreover, different workpiece and tool geometries and machining strategy were chosen with the aim improving the reliability of the measurements.

Test description
The geometry of the workpiece consisted of a series of grooves machined in brass by means of parallel passes with the 0.2 mm flat end mill. The tool passes were taken at Z levels from +5 μm to -5 μm from the flat surface generated with a ∅ 6 mm flat end mill. The incremental depth was 1 μm. An additional pass at -5 μm was generated before all the others and constituted a reference useful in order to check for the influence of the tool wear on the subsequent grooves. The sketch in fig. 29 shows the operation.
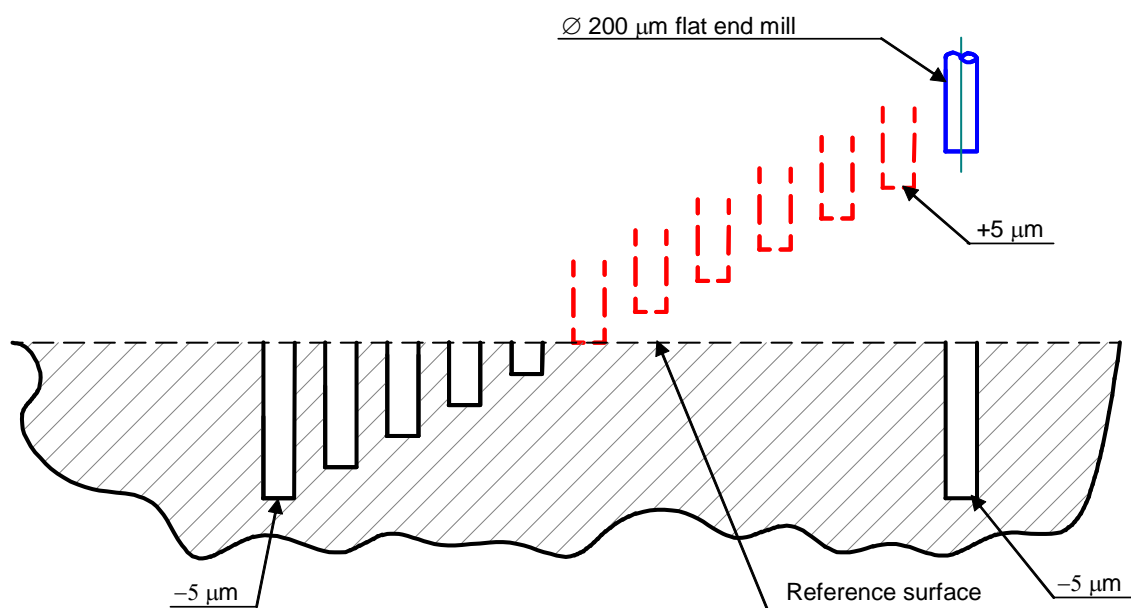

Fig. 29 Sketch representing the layout of the surfaces to be generated during the test.

The parallel tool passes followed one another from right to left and, ideally, only in the first and in the last five passes the tool should have engaged the material. The details of the machining sequence are as follows:

Generation of reference surface :   Tool: flat end mill OSG FXS-EMSS ∅6 mm, 6 flutes
                                         f = 400 mm/min
                                         n = 6350 rpm

Generation of the grooves: Tool: ball nose end mill OSG WX-LN-EDS ∅ 0.2 x 1.5, 2 flutes
                                         f = 265 mm/min
                                         n = 31831 rpm

Avoidance of the misalignment problem between the two tools during tool length correction was obtained performing the tool length correction of the ∅ 6 mm end mill at location X=0 Y=0 (the tool is large enough to avoid contact in the area of the tip interested by the scratch) and that for the ∅ 0.2 mm end mill at location X=-2.9 mm Y=0 mm.

10 profiles on the machined surface were measured with a contact profilometer Taylor-Hobson RTH Talysurf 5-120 with a sampling distance of 5 μm in X direction and 10 μm in Y direction. Fig. 30 reports a representative profile and a 3D view of the measured surface.
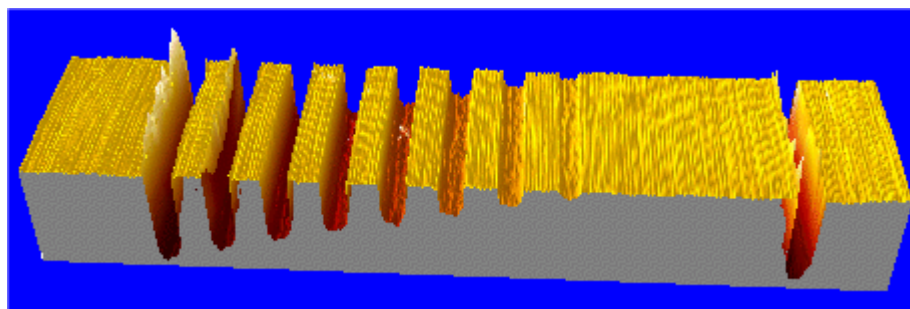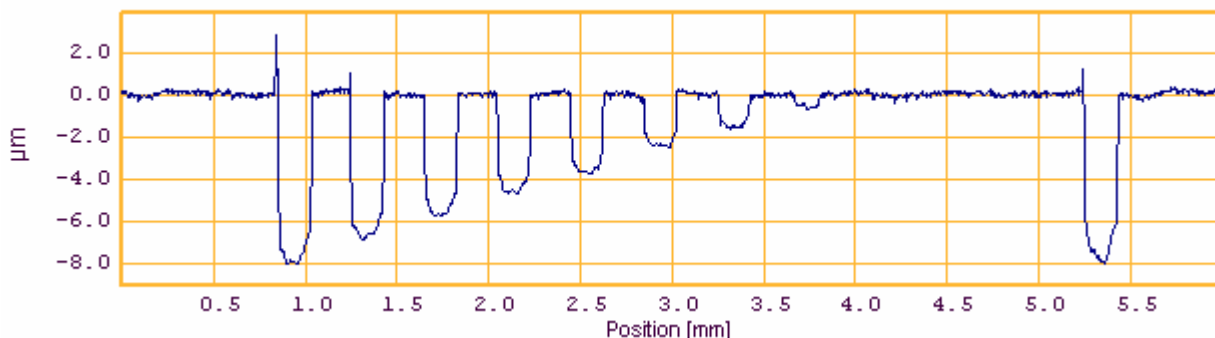

Fig. 30 Representative profile of the machined pattern and 3D view of the machined surface.

Results
As is visible both in the profile and the 3D view reported above, 8 passes as well as the reference one have engaged the material, therefore overengagement is still present.

However, the depth error is quite constant over all the engaged grooves and the average value is only 2.8 μm, ranging from 2.6 μm to 3.1 μm. This is shown in fig. 31.

An accurate observation of the profile of the grooves shows that their bottom is not flat but concave and that the concave part corresponds to 1 to 2 μm in axial depth. The profile of the bottom of the grooves, as it appears in fig. 30, is misleading, since there, it looks almost a half circle. In fact this effect is produced by the enormous difference between the scales in the two axes, having a ratio of 200 and necessary in order to appreciate the profile characteristics. The profile is actually characterized by a small slope which corresponds to the small chamfer at the extremity of the micro flat end mills, as shown by SEM picture reported in fig. 31.
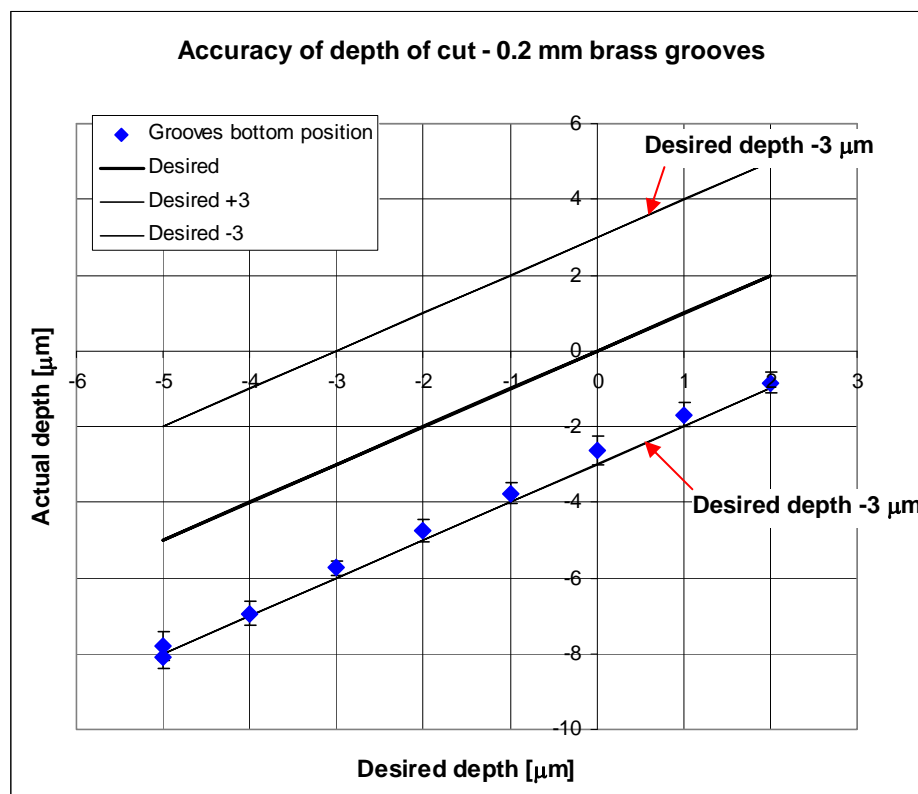

Fig. 31   Measured depth of the machined grooves. Each point represents the average of 10 parallel profiles; the small error bars correspond to ±2*STD.

A further consideration is that during the tool length correction of the ∅ 6 mm flat end mill, the zero point in Z could vary by as much as 3 μm due to the axial run out of the different teeth. The actual position of the reference surface depends, therefore, on which of the 6 teeth was used for the tool length correction. In all the tests, the tooth producing the maximum tool length was chosen for the tool length correction. However in this respect, a ball nose end mill would allow a more precise correction, since all the cutting edges meet at the tool tip, which is also the lowest point of the tool.

Conclusions

The main result of this test is that the axial depth of cut, when tool wear effect are not present, is proved to be in control within ±3 μm, and if BUE could be avoided, the control would further improve. The chamfer at the end of the tool is responsible for the slope of the walls of generated grooves. Axial run out of the larger tool teeth can account for up to

3 μm. This last problem could be avoided using a large ball nose end mill for the generation of the reference surface.

7.9   Second test workpiece in brass for verification of the achieved depth of cut accuracy without tool wear effects.

This test constitutes the last of the test series for axial depth of cut optimization, carried out with the set up described in the previous chapters of this document. The objective of the test is to eliminate the error due to the axial run out of the large end mill by using a ball nose end mill for the generation of the reference surface. The pattern generated is the same as for the previous test and only the differences will be reported here.

Test description

The details concerning the machining sequence are:

Generation of reference surface :   Tool: flat end mill OSG FXS-EBM ∅ 6 mm, 4 flutes
                                         f = 1000 mm/min
                                         n = 15915 rpm

Generation of the grooves: Tool: ball nose end mill OSG WX-LN-EDS ∅ 0.2 x 1.5, 2 flutes
                                         f = 265 mm/min
                                         n = 31831 rpm

Tool correction positions were X=2.0 mm Y=0 for the ∅ 6 mm ball nose end mill and X=2.1 mm Y=0 for the ∅ 0.2 mm flat end mill. 10 profiles on the machined surface were measured with a contact profilometer Taylor-Hobson RTH Talysurf 5-120 with a sampling distance of 2 μm in X direction and 10 μm in Y direction.
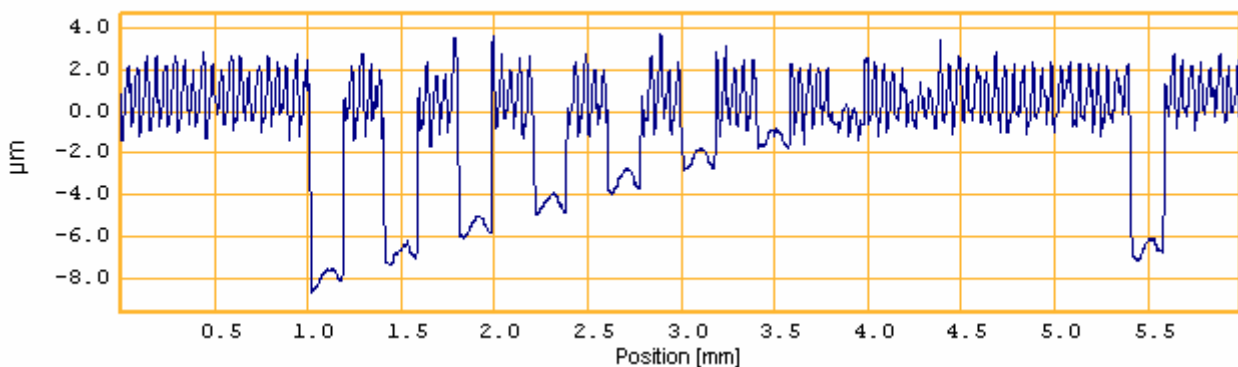

Fig. 32 Representative profile of the machined pattern.

Results

The representative profile reported in fig. 32 shows that 7 grooves plus the reference one have fully engaged the material, and other two have engaged with the peaks of the roughness profile of the reference surface. Due to the ploughing and smearing effect of the large ball nose end mill on the soft workpiece material, the roughness on the reference surface is much larger than that calculated for the cutting parameters used. However,

considering that the vertical alignment has been performed on the tip of the ball nose end mill, the bottom of the regular grooves produced on the reference surface should be the vertical reference for the offset of the profile for the groove depth measurement. The representative profile in fig. 32 is offset of 1 μm in fig. 33.

Applying such an offset to each measured profile, the measurement results are those shown in fig. 34.
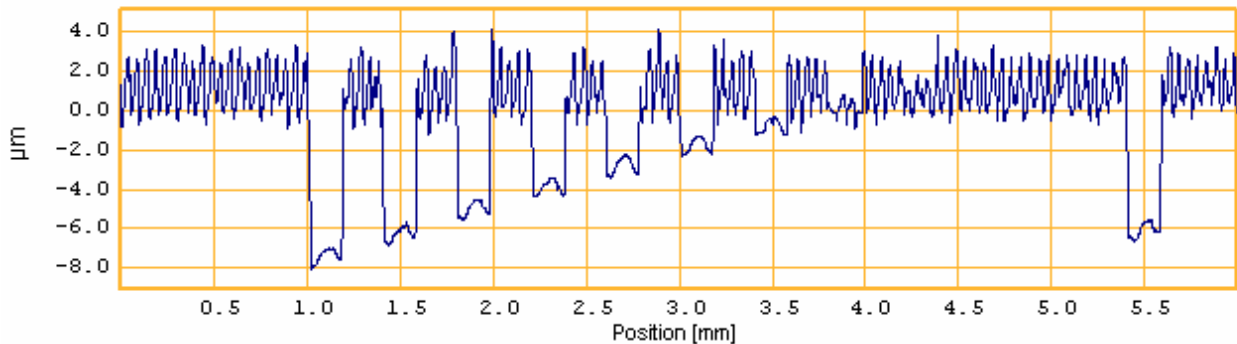

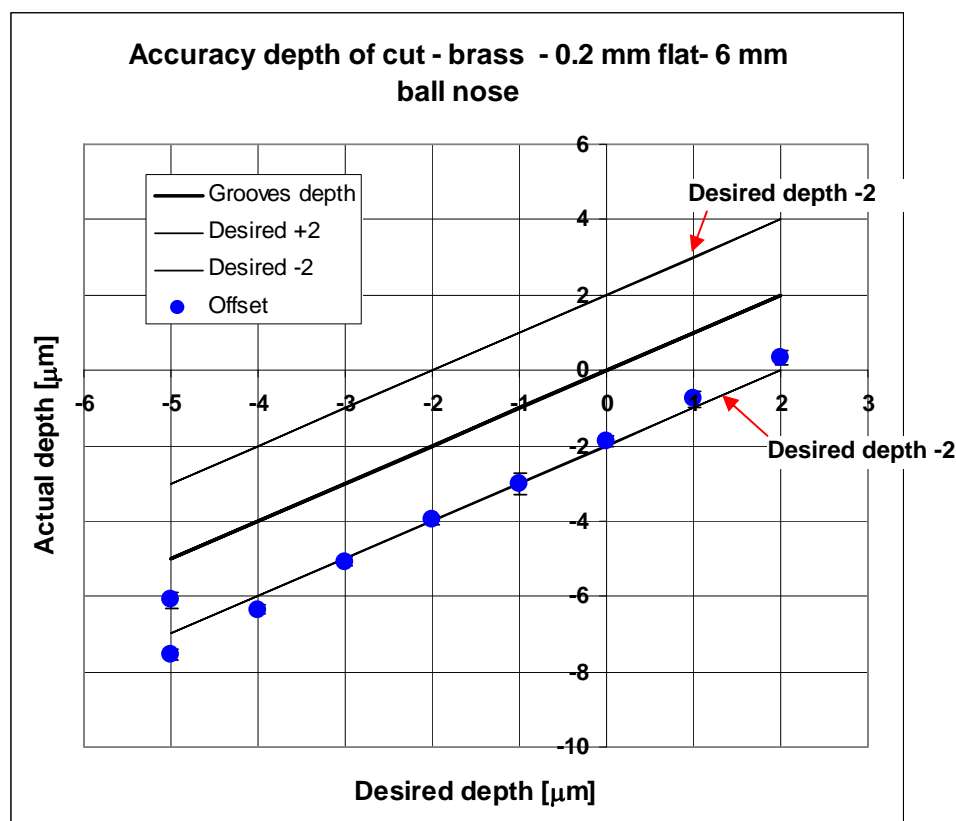Fig. 33 Representative profile of the machined pattern offset in vertical (Z) direction.

Fig. 34 Measured depth of the machined grooves. Each point represents the average of 10 parallel profiles; the small error bars correspond to ±2*STD.

The average error on the depth of cut was 1.93 μm ranging from 1.09 μm to 2.54 μm and the standard deviation was less than 0.15 μm for each grooves (10 profiles have been measured). The improvement obtained by elimination of the effect of the axial run out of the large end mill was negligible, probably because of the rough reference surface produced which did not allow a good alignment. The depth of cut error in the last two tests

has been less than 3 µm and constitutes the main result of this optimization study. However, BUE is believed to be present because the cutting speed is very low at any point of the micro end mills, particularly for a soft material like brass. This could easily be responsible for 5 µm of increase in depth of cut and would disguise any further improvement in the control of the tool position in Z direction.

8   Summary and conclusions

The series of tests described in the previous chapter 7 has allowed identification of the main causes of error on the axial depth of cut in micromilling, and estimation of their error contribution. Each of them has provided a little more insight on the process and interaction between the influencing factors and, in turn, has enabled some progress in the working procedure optimization process. The tests described above could be classified in such a way that, a visualization of the areas where optimization has been achieved, is depicted. This is shown in fig. 35, which refers to the sketch shown in fig. 4.
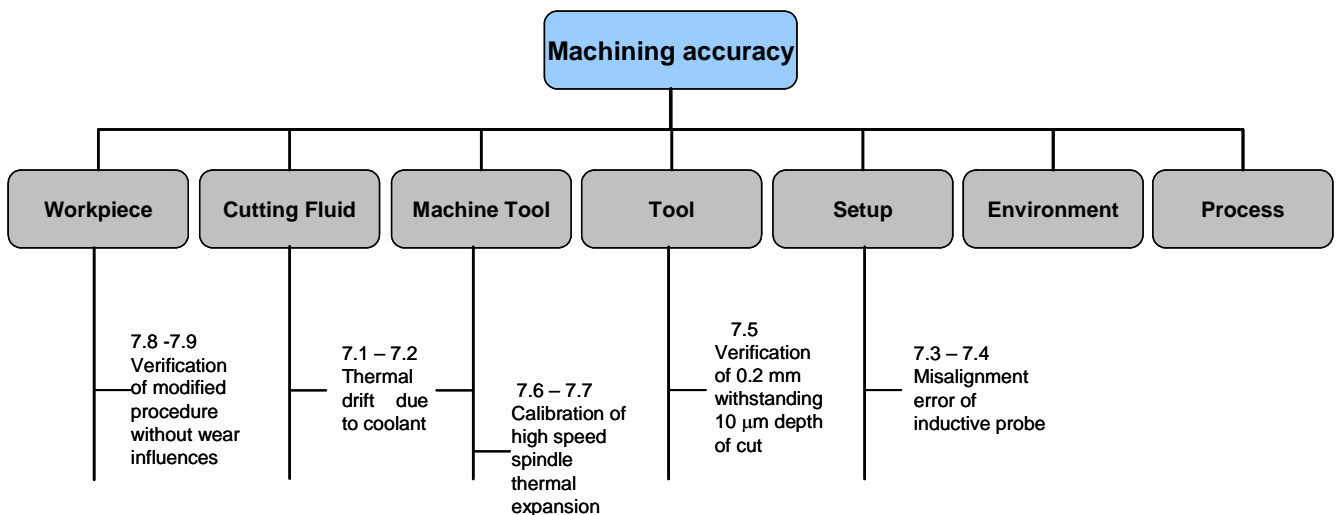
Fig. 35   Relationship between Machining Accuracy, Independent Process Parameters and optimization tests.

The achieved accuracy of control of the axial depth of cut, which is of the utmost importance when milling with end mills having very little strength and stiffness, is in the order of 3 µm. Although this is an empirical optimization, it should be regarded as a very good result when compared with data available in the literature for conventional machining. In fact, this result has been achieved only by improving the working procedure, while most of other works required either expensive design solutions or modifications of the machine tool, or continuous monitoring and online adjustment by use of sophisticate software tools as neural networks. The total depth of cut error initially affecting the machining operations was not known, but can be extrapolated by summing up all the error reductions obtained in the different optimization steps described above. This is shown in table 5.

Contribution	Contribution value [μm]
Coolant drift	+8.5
Inclination of the inductive probe tip (roughing tool Ø 6 mm finishing tool Ø 0.2 mm)	+5
High speed spindle thermal drift (worst case: highest speed from room temp. to steady state temp. Extrapolated value)	+20
Axial run out of roughing tool	±3
Total (worst case)	**+36.5**
Depth of cut error after optimization	**±3**

Tab. 5 Magnitude and direction of the main contributions to the axial depth of cut error (difference with the optimized procedure) and residual error after optimization. + indicates an increase of the depth of cut.

According to table 5 the maximum error (excluding the contribution from machine tool distortions during the one hour warm up cycle) was 36.5 μm (which would be already good if compared to normal situations where the main spindle is rotated). This fully explains the systematic breakage of the 0.2 mm end mills when machining surfaces at low inclination angle. With the optimized procedure, the error has been reduced to 1/12 of the initial one. The machining operations that were initially impossible, and have required this optimization study, have been successfully carried out using the optimized procedure, showing the goodness of the approach employed, based on the assumption of reproducible machining conditions and repeatable machine tool behaviour. That is the temperature-elongation curves are repeatable and reliable. High tool wear was still affecting the machining, particularly at low inclination angle. This was expected particularly for the low cutting speed involved and is the subject of a separate report.

References

[1]   M. Weck, P. McKeown, R Bonse, U. Herbst, 1995, *Reduction and Compensation of Thermal Errors in Machine Tools*, Annals of the CIRP Vol. 44/2, pp. 589-598.

[2]   J. Bryan, 1990, *International Status of Thermal Error Research (1990)*, Annals of the CIRP Vol. 39/2, pp. 645-656.

[3]   H.J. Pahk, S.W. Lee, 2002, *Thermal Error Measurement and Real Time Compensation System for the CNC Machine Tools Incorporating the Spindle Thermal Error and the Feed Axis Thermal Error*, Int. J. Advanced Manufacturing Technology, (2002) 20, pp. 487-494.

[4]   D.S. Lee, J.Y. Choi, D.H. Choi, 2003, *ICA based thermal source extraction and thermal distortion compensation method for a machine tool*, Int. J. Machine Tools & Manufacture, 43 (2003), pp. 589-597.

[5]   G. Spur, E. Hoffmann, Z. Paluncic, K. Benzinger, H. Nymoen, 1988, *Thermal Behaviour Optimization of Machine Tools*, Annals of the CIRP Vol. 37/1, pp. 401-405.

[6]   S.C. Veldhuis, M.A. Elbestawi, 1995, *A Strategy for the Compensation of Errors in Five-Axis Machining*, Annals of the CIRP Vol. 44/1, pp. 373-.377.

[7]   S. Sartori, G.X. Zhang, 1995, *Geometric Error Measurement and Compensation of Machines*, Annals of the CIRP Vol. 44/2, pp. 599-609.

[8]   S. Fraser, M.H. Attia, M.O.M. Osman, 1999 *Modelling, Identification and Control of Thermal Deformation of Machine Tool Structures, Part3: Real Time Estimation of Heat Sources*, J. Manufacturing Science and Engineering, Vol. 121, pp. 501-508.

[9]   S. Fraser, M.H. Attia, M.O.M. Osman, 1999 *Modelling, Identification and Control of Thermal Deformation of Machine Tool Structures, Part4: A Multi-Variable Closed-Loop Control System*, J. Manufacturing Science and Engineering, Vol. 121, pp. 509-516.

[10]   S. Fraser, M.H. Attia, M.O.M. Osman, 1999 *Modelling, Identification and Control of Thermal Deformation of Machine Tool Structures, Part5: Experimental Verification*, J. Manufacturing Science and Engineering, Vol. 121, pp. 517-523.

[11]   E. Budak, Y. Altintas, E.J.A. Armarego, 1996 *Prediction of Milling Force Coefficients From Orthogonal Cutting Data*, J. Manufacturing Science and Engineering, Transaction of the ASME, Vol. 118, pp. 216-224.